JVI Accepts, published online ahead of print on 11 August 2010
J. Virol. doi:10.1128/JVI.00431-10

Quantitative Proteomic Analyses of Influenza virus-Infected Cultured Human Lung Cells

[1,2,3]Kevin M. Coombs*, [1,2]Alicia Berard, [1,2]Wanhong Xu, [2]Oleg Krokhin, [2]Xiaobo Meng, [2]John P. Cortens, [1,4]Darwyn Kobasa, [2,5]John Wilkins, and [6]Earl G. Brown

[1] Department of Medical Microbiology, Faculty of Medicine, University of Manitoba, Winnipeg, Manitoba R3E 0J6 Canada;
[2] Manitoba Centre for Proteomics & Systems Biology, Room 799, 715 McDermot Avenue, Winnipeg, Manitoba, Canada R3E 3P4 Canada;
[3] Manitoba Institute of Child Health, Room 513, John Buhler Research Centre, 715 McDermot Avenue, Winnipeg, Manitoba R3E 3P4 Canada;
[4] Respiratory Viruses Program, National Microbiology Laboratory, Public Health Agency of Canada, Winnipeg, Manitoba R3E 3R2 Canada;
[5] Department of Internal Medicine, Faculty of Medicine, University of Manitoba, Winnipeg, R3E 3P4 Canada;
[6] Department of Biochemistry, Microbiology, and Immunology, and Emerging Pathogens Research Centre, University of Ottawa, Ottawa, Ontario, K1H 8M5 Canada

* Corresponding Author:
Kevin Coombs
Manitoba Centre for Proteomics and Systems Biology
Room 799 John Buhler Research Centre
715 McDermot Avenue
Winnipeg, MB R3E 3P4
(v)204.789.3976
(f)204.480.1362
kcoombs@cc.umanitoba.ca

Condensed Title: Influenza virus quantitative Proteomics

Keywords: RNA virus; Virus infection; Host cell alterations; Mass spectrometry; Liquid chromatography; Bioinformatics

Abstract: 186 words

Text: 6509 words

Figures: 5

Tables: 3

Supplementary Tables: T1 – T2

Abstract

Because they are obligate intracellular parasites, all viruses are exclusively and intimately dependent upon host cells for replication. Viruses, in turn, induce profound changes within cells, including apoptosis, morphological changes, and activation of signaling pathways. Many of these alterations have been analyzed by gene arrays, which measure the cellular "transcriptome". Until recently, it has not been possible to extend comparable types of studies to globally examine all the host cellular proteins, which are the actual effector molecules. We have used SILAC (stable isotope labeling by amino acids in cell culture), combined with high-throughput 2-D HPLC/mass spectrometry, to determine quantitative differences in host proteins after infection of human lung A549 cells with human influenza virus A/PR/8/34 (H1N1) for 24 hours. Of the 4689 identified and measured cytosolic protein pairs, 127 were significantly up-regulated at >95% confidence, 153 were significantly down-regulated at >95% confidence, and a total of 87 proteins were up-regulated or down-regulated more than 5-fold at >99% confidence. Gene ontology and pathway analyses indicated differentially-regulated proteins included those involved in host cell immunity and antigen presentation, cell adhesion, metabolism, protein function, signal transduction, and transcription pathways.

Introduction

Influenza A virus (FLUAV), a member of the family *Orthomyxoviridae,* is a small enveloped virus with a genome consisting of 8 segments of negative-sense single stranded RNA that encodes for 10-11 proteins depending on the strain (56). The segmented genome and highly error-prone viral replication lead to enormous genetic plasticity, mediated by nucleotide or genome segment exchange, termed genetic drift and genetic shift, respectively. Genomic changes control the differences in virulence and host range seen among FLUAV isolates. FLUAV are serologically categorized by 2 surface proteins: hemagglutinin (HA), of which there are currently 16 types (H1 – H16) and neuraminidase (NA), of which there are currently 9 types (N1 – 9) (56). Virtually every possible H/N combination has been found in water fowl (2,46), the generally-accepted reservoir, but only a few H/N types have circulated in humans; H1N1 (1918 "Spanish Flu" and the current pandemic H1N1 2009 strains), H2N2 and H3N2. A number of anti-viral strategies, including vaccines and small molecule inhibitors, have been developed to combat this virus, but its genetic plasticity often leads to resistance to virus-targeted anti-viral strategies. Because of its small genome, the virus, like other viruses, is an obligate parasite and must make extensive use of host cell machinery. Thus, an alternate anti-viral strategy would be to better understand the critical host factors that are influenced and required by the virus for its efficient propagation.

While a cell's genome generally remains relatively constant (except for certain epigenetic events; see (28,33) for reviews), the cell's proteome (the total protein repertoire, including how any given protein may be co-translationally or post-translationally modified) varies greatly due to its biochemical interactions with the genome, as well as the cell's interactions with the environment. A cell's protein expression is dependant on the location of the cell, different stages of its life cycle, and different environmental conditions. In the case of viruses, which require the host cell's machinery and metabolism to replicate, the cell's proteome also reflects the specific alterations of the pathways induced by virus infection.

Previous analyses of how cells respond to influenza virus infection have used microarray technologies which measure the cellular "transcriptome" (for example: (6,30,45)). However, there frequently is little concordance between microarray and protein data (6,52,71), partly because mRNA levels cannot provide complete information about levels of protein synthesis or extents of post-translational modifications. Thus, proteomic analyses have also been employed to better understand host alterations to virus infection. Vester et al used 2D difference in gel electrophoresis (2D-DIGE) and identified 8 significantly altered host proteins in each of influenza virus A/PR/8/34 (H1N1)-infected canine MDCK and human A549 cells (72) and Liu and colleagues used a similar approach to identify about 25 significantly altered host proteins in avian influenza A/Hong Kong/108/2003 (H9N2)-infected human gastric carcinoma cells (48).

There have been a number of significant improvements in quantitative proteomic analyses, particularly in areas of non-gel-based studies, such as ICAT (isotope coded affinity tags; see (11,35,39) for some examples), iTRAQ (isobaric tags for relative and absolute quantitation; see (12,20,61,77) for examples) and SILAC (stable isotope labeling by amino acids in cell culture; see (15,16,27,34,55) for examples). There also have been improvements in peptide fractionation (22,67). Therefore, we decided to apply newer quantitative approaches to more fully probe the richness of influenza virus-infected host cell proteomes to attempt to identify additional potential anti-viral targets. We chose SILAC, using $^{12}C_6$-Lys and $^{12}C_6{}^{14}N_4$-Arg ("light"; **L**), and $^{13}C_6$-Lys and $^{13}C_6{}^{15}N_4$-Arg ("heavy"; **H**), because virtually every tryptic peptide is expected to contain an **L** or **H** label, thereby providing increased protein coverage, **L** and **H** samples are mixed together early in the process, thereby reducing sample-to-sample variability, and other such studies succeeded in identifying and quantitatively measuring up to several thousands of proteins (7,15,34,62). We succeeded in the current study in identifying and measuring nearly 4700 cytosolic host proteins, of which 127 were significantly up-regulated, including proteins involved in acetylation, cell structure, defense responses, protein binding, and responses to stress, stimulus and virus; and 153 proteins, including those involved in alternative splicing, localization, transport, protein binding, and nucleoside, nucleotide and nucleic acid metabolism that were significantly down-regulated.

Experimental Procedures

Cells and viruses

Viruses

Influenza virus strain A/PR/8/34 (H1N1) was grown in embryonated hens eggs from laboratory stocks, and chorioallantoic fluid was harvested, aliquotted, and titered in MDCK cells by standard procedures (8). Additional stocks were made by recombinant means to exclude chorioallantoic fluid effects (53).

Cells

Human lung A549 cells were routinely cultured in Dulbecco's modified MEM (DMEM) supplemented with non-essential amino acids, sodium pyruvate, 0.2% (w/v) glucose, 10% Fetal bovine serum (FBS; Intergen), and 2 mM l-glutamine. Cells were maintained as monolayers in 10% CO_2 and were passaged by trypsinization 2 – 3 times each week. For SILAC labeling, cells were grown in DMEM media provided with a SILAC^{TM} Phosphoprotein Identification and Quantification Kit (Invitrogen Canada Inc.; Burlington, Ontario), supplemented as above (except without non-essential amino acids), and with 10% dialyzed FBS (Invitrogen Canada Inc.; Burlington, Ontario), plus 100mg each of "light" (**L**) or "heavy" (**H**) l-lysine and l-arginine per liter of D-MEM.

Infection

Once the cells had grown through six doublings, **L** cells in T25 and T75 flasks were infected with A/PR/8/34 at a multiplicity of infection (MOI) of 7 plaque forming units (PFU) per cell. An equivalent number of **H** cells were mock infected as control. Cells were overlaid with appropriate media and cultured for various periods of time. Infections were carried out multiple times over several months.

Photomicrography

Infected and mock-infected cells in the T25 flask were examined microscopically for cytopathic effect (CPE) at 0, 12, 18, 24, 30, and 36 hours post-infection with a Nikon TE-2000 and cells were photographed with a Canon-A700 digital camera. Images were imported into Adobe and slight adjustments made in brightness and contrast, but which did not alter image context with respect to each other.

Cell Fractionation

At 24 hours post-infection, **L** and **H** cells in the T75 flasks were collected and counted. To verify infection status of each culture, aliquots of all cultures were saved for virus titration and for Western blotting (see below). For comparative SILAC assays, equivalent numbers of **L** and **H** cells were mixed together, and the mixed cells were washed 3× in >50 volumes of ice-cold Phosphate Buffered Saline (PBS). For assays to confirm differential infection status, infected and mock-infected cells were processed separately. In assays destined for SDS-PAGE separations, washed cells were swollen in hypotonic buffer (10mM NaCl, 10mM HEPES, pH 7.5, supplemented with 1.1µM pepstatin A) for 30 minutes on ice, then cells lysed by 20 passages through a 30ga needle. Lysis was confirmed microscopically and nuclei and insoluble membranes pelleted at 5000xg for 10 minutes. The supernatant was saved as "cytosol". The nuclei and crude membranes were re-suspended in 200µl of 0.5% NP-40, incubated on ice for 30 minutes, and nuclei removed by pelleting at 5000xg for 10 minutes. The "crude membranes" (supernatant) were transferred to a fresh microfuge tube; and electrophoresis sample buffer was added to each of the three fractions (nuclear pellet, crude membranes and cytosol) which were then frozen at -80^{o}C until further processing took place. In assays destined for liquid chromatographic separations, washed cells were lysed with 0.5% NP-40, supplemented with 1.1µM pepstatin A, incubated on ice for 30 minutes, and nuclei removed by pelleting at 5000xg for 10 minutes. The cytosol and soluble membranes (supernatant) were transferred to fresh microfuge tubes; and the two fractions (nuclear pellet and supernatant) were frozen at -80^{o}C until further processing took place.

Immunoblotting

Aliquots of unlabeled, and **L**- and **H**-labeled, infected and mock-infected cells were separately harvested, dissolved with 0.5% NP-40 as described above, and cytosolic fractions collected, mixed with SDS electrophoresis sample buffer, heated to 95°C for 5 minutes, and resolved in 5-15% mini gradient SDS-PAGE (6.0 × 10.0 × 0.1cm) at 180V for 50min (until the bromophenol blue tracking dye was at the gel bottom), and proteins transferred to PVDF. The PVDF membranes were briefly stained with Ponceau to confirm protein transfer, blocked with 5% skim milk, and probed with various antibodies. Primary antibodies were: mouse anti-influenza NP protein (74), α-GAPDH, α-Vimentin, α-β-2-microglobulin, α-Vasp, rabbit anti-Actin, α-Rock2, α-Akt, α-cytokeratin 10, α-Bid, and goat anti-Parp. Secondary antibodies were Alexa488-conjugated goat anti-mouse for NP and GAPDH, Alexa488-conjugated goat anti-rabbit for actin, or appropriate HRP-conjugated rabbit anti-mouse, goat anti-rabbit or rabbit anti-goat for all other proteins. HRP was detected by enhanced chemiluminescence, and film and fluorescent secondary antibodies were visualized, and band intensities measured, with an Alpha Innotech FluorChem®Q MultiImage® III instrument.

Protein digestion

Protein content in the cytosolic and soluble membrane fractions collected as described above was determined using a BCA™ Protein Assay Kit (Pierce; Rockford, IL) and BSA standards. After protein concentration determinations, samples were diluted with freshly made 100mM ammonium bicarbonate to provide concentrations of ~1 mg/ml and pH ~8. Three hundred µl of each sample (~300 µg of protein) were reduced, alkylated and trypsin-digested using the following procedure. Thirty µl of freshly prepared 100mM dithiothreitol (DTT) in 100mM ammonium bicarbonate was added. The samples were then incubated for 45 minutes at 60°C. 30 µl of freshly prepared iodoacetic acid (500 mM solution in 100mM ammonium bicarbonate) was added to each tube and the tubes were then incubated for 30 min at room temperature, in the dark. Finally, 50 µl of 100mM DTT solution was added to quench the excess

iodoacetic acid. Samples were digested overnight at 37°C with 6 μg of sequencing grade trypsin (Promega, Madison, WI). The samples were lyophilized and stored at -80°C.

Peptide fractionation using 2D RP HPLC

A newly developed orthogonal procedure (32,67) was employed for 2D RP (reversed-phase) high pH – RP low pH peptide fractionation. Lyophilized tryptic digests were dissolved in 200 μl of 20 mM ammonium formate pH 10 (buffer A for first dimension separation), injected onto a 1×100mm XTerra (Waters, Milford, MA) column and fractionated using a 0.67% acetonitrile per minute linear gradient (Agilent 1100 Series HPLC system, Agilent Technologies, Wilmington, DE) at a 150 μL/min flow rate. Sixty 1-min fractions were collected (covering ~40 % acetonitrile concentration range) and concatenated using procedures described elsewhere (22,67); the last 30 fractions were combined with the first 30 fractions in sequential order (i.e. #1 with #31; #2 with #32, etc.). Combined fractions were vacuum-dried and re-dissolved in buffer A for the second dimension RP separation (0.1% formic acid in water).

A splitless nano-flow Tempo LC system (Eksigent, Dublin, CA) with 20 μL sample injection via a 300μm×5mm PepMap100 pre-column (Dionex, Sunnyvale, CA) and a 100μm×200mm analytical column packed with 5μm Luna C18(2) (Phenomenex, Torrance, CA) were used in the second dimension separation prior to MS analysis. Both eluents A (water) and B (acetonitrile) contained 0.1 % formic acid as an ion-pairing modifier. A 0.33 % acetonitrile per minute linear gradient (0-30% B) was used for peptide elution, providing a total 2-hour run time per fraction in the second dimension.

Mass Spectrometry, Bioinformatics, and Data Mining

A QStar Elite mass spectrometer (Applied Biosystems, Foster City, CA) was used in a data-dependent MS/MS acquisition mode. One-second survey MS spectra were collected (m/z 400-1500) followed by MS/MS measurements on the 3 most intense parent ions (80 counts/sec threshold, +2 - +4 charge state, m/z 100-1500 mass range for MS/MS), using the manufacturer's "smart exit" (spectral quality 5) settings.

Previously targeted parent ions were excluded from repetitive MS/MS acquisition for 60 sec (50 mDa mass tolerance). Protein Pilot 2.0 (Applied Biosystems) software was used for protein identification and quantitation. Raw data files (30 in total for each run) were submitted for simultaneous search using standard SILAC settings for QStar instruments. Proteins for which at least 2 fully trypsin digested **L** and **H** peptides were detected at >99% confidence were used for subsequent comparative quantitative analysis. Raw MS data files were analyzed by Protein Pilot®, version 2.0, using the non-redundant human gene database. Proteins, and their confidences and **L:H** ratios, were returned with gi accession numbers.

Differential regulation within each experimental dataset was determined by normalization of each dataset, essentially as described (43). Briefly, every **L:H** ratio was converted into $\log_2$ space to determine geometric means and facilitate normalization. The average $\log_2$ **L:H** ratios and standard deviation of the $\log_2$ **L:H** ratios were determined for each dataset, both before, and after, computational removal of the few (up to 12) significant outliers found in a few datasets. Every proteins' $\log_2$ **L:H** ratio was then converted into a z-score, using the formula:

$$\text{Z-score } (\sigma) \text{ of [b]} = \frac{\text{Log}_2\textbf{L:H}[\text{b}] - \text{Average of } (\log_2 \text{ of each member, a}\ldots.\text{n})}{\text{Standard deviation of } (\log_2 \text{ of each member, a}\ldots.\text{n})}$$

where "b" represents an individual protein in a dataset population a….n, and z-score is the measure of how many standard deviation units (expressed as "σ") that protein's $\log_2$ **L:H** ratio is away from its population mean. Thus, a protein with a z-score > 1.645σ indicates that protein's differential expression lies outside the 90% confidence level, > 1.960σ indicates outside the 95% confidence level, 2.576σ indicates 99% confidence, and 3.291σ indicates 99.9% confidence. Z-scores >1.960 were considered significant. Gi numbers of all significantly regulated proteins were converted into HGNC identifiers by Uniprot (http://www.uniprot.org/) and HGNC terms were submitted to and analyzed by the DAVID bioinformatic suite at the NIAID, version 6.7 (19,41) and gene ontologies examined with the "FAT" datasets. The gi numbers were also submitted to, and pathways constructed with, Ingenuity Pathway Analysis software (IPA®).

Results

Kinetics of Influenza virus-induced cytopathology in cultured A549 cells.

One of the key parameters for determining virus-induced alterations, and in separating such alterations from general stress responses related to cell death late in infection, would be to determine when cytopathic effects (CPE) are manifested in the model system. Accordingly, we initially infected our A549 cultured human lung cells with Influenza strain A/PR/8/34 (H1N1; "PR8") at multiplicities of 7 plaque forming units (PFU) per cell (>99% of cells are initially infected as predicted by the Poisson distribution) and microscopically monitored for cell viability and CPE over time. Cells infected with PR8 and cultured for 24h or less demonstrated no detectable CPE, there was minimal CPE detectable at 30h post-infection (hpi), and CPE was readily apparent at later time points (Fig. 1). Therefore, in subsequent experiments, A549 cells were infected with the same MOI of PR8, cultured for 24h, and processed in order to allow the virus to exert maximal effect without demonstrable CPE.

2D-HPLC provides more extensive protein identification than 1D SDS-PAGE/1D-LC-ESI-MS.

Eukaryotic cells possess highly complex proteomes and peptide sample complexity must be reduced prior to MS-based interrogation (reviewed in (23,75)). There are several strategies for reducing sample complexity. We initially evaluated and compared gel-based purification of intact cellular proteins to HPLC purification of digested peptides. Equivalent numbers of PR8-infected $^{12}C_6$-Lys, $^{12}C_6{}^{14}N_4$-Arg (SILAC **L**ight) and mock-infected $^{13}C_6$-Lys, $^{13}C_6{}^{15}N_4$-Arg (SILAC **H**eavy) A549 cells were mixed together and various purification methods were tested. Initially, mixtures of **L**- and **H**-labeled entire cells were dissolved in electrophoresis sample buffer, resolved in a single gel lane of a 5-15% mini SDS-PAGE gel, the entire gel lane cut into 24 slices, and each slice processed by in-gel trypsin digestion. Peptides were extracted and processed as detailed more fully in Experimental Procedures by liquid

chromatography/electrospray ionization mass spectrometry (LC/ESI-MS); this resulted in the identification of about 300 pairs of proteins (data not shown).

We then fractionated mixed **L/H** cells as described in Experimental Procedures to generate crude "cytosolic", "membrane", and "nuclear" fractions, each of which were separately resolved by 1-D SDS-PAGE/1D-LC-ESI-MS as described above. Approximately 250 – 550 **L/H** protein pairs were detected and measured in each fraction in each of 2 biologic replicates, using stringent protein identification criteria of 2 complete **L** and **H** tryptic peptides and identification confidence ≥ 99% (Table 1). There were some common proteins found in different fractions, such that compilation of both 1-D SDS-PAGE/1D-LC-ESI-MS analyses identified 1002 pairs of proteins in the combined cytosolic and membrane fractions (Fig. 2A). As an alternate strategy, equivalent **L/ H** cell mixtures were washed, lysed with 0.5% NP-40 to obtain cytosolic and membrane fractions, proteins digested with trypsin, and peptides processed for 2D HPLC/ESI-MS as detailed in Experimental Procedures. Analyses of 2 separate biological replicates processed this way identified more than 2100 pairs of proteins. More than 500 of the identified protein pairs were common to both the 1-D SDS-PAGE/1D-LC-ESI-MS and the 2D-HPLC/ESI-MS methods, and many proteins were also detected in the nuclear fractions (Fig. 2A).

Having established that 2D HPLC/ESI-MS identified more than twice as many protein pairs as 1D SDS-PAGE/1D-LC-ESI-MS, we then performed 2 technical 2-D HPLC/ESI-MS analyses on an additional biological experiment. These technical replicates identified a total of 3173 unique cytosolic proteins (Table 1), of which 2044 were common to both replicates. Comparisons of each of these 2044 common proteins' Log_2 ratios showed a correlation of $r^2 = 0.660$ (data not shown), indicating most of the commonly identified proteins had similar **L:H** ratios in each technical replicate. Ten of the 2044 proteins did not behave similarly in both replicate runs such that they differed in significance or direction of regulation. One protein (MGC2477), was measured as significantly up-regulated 18-fold in one technical replicate but down-regulated almost 2-fold in the other run. Nine other proteins appeared to be significantly up- or down-regulated in one run (defined as described above) but were slightly regulated in the opposite direction in the other replicate. These 10 proteins were included in subsequent statistical

analyses, but because we could not confidently establish whether each was up- or down-regulated, we did not include them in lists of up- and down-regulated proteins or in subsequent gene ontology and pathway analyses.

Influenza virus infection induces significant up- and down-regulation of numerous cellular proteins.

Combination of all 2D-LC-identified proteins with all 1D-SDS-PAGE/1D-LC-identified proteins resulted in identification and measurement of 4817 total unique protein pairs. Inspection of each protein's $\log_2$ distribution indicated variability in each dataset's mean $\log_2$ value and in each dataset's $\log_2$ standard deviation (Fig. 2C; Table 1). Thus, every proteins' **L:H** ratio was converted into a z-score as described in Materials and Methods to allow inter-experiment comparisons.

Stratification of each protein's **L:H** ratio and its z-score from each experimental run indicated that numerous proteins were identified in each experiment that could be considered significantly regulated. For example, of the 248 proteins identified in the first SDS-PAGE/LC-prepared cytosol sample, 8 were upregulated at 95% confidence and each of these was also upregulated at 99.9% confidence (Table 1). Six proteins in the same dataset were down-regulated at 95% confidence, but only one of these proteins was also down-regulated at 99.9% confidence. Inspection of protein **L:H** ratios and z-scores indicated that most proteins differentially regulated at >95% confidence had **L:H** ratios altered by > 1.6-fold and most proteins differentially regulated at >99% confidence had **L:H** ratios altered by > 2.2-fold. However, a number of proteins with **L:H** ratios in the 0.667 – 1.500 range also had significant z-scores. For example, a protein might have an **L:H** ratio of 1.2 but be considered significant if it was a member of a population with a negative mean $\log_2$L:H and a small standard deviation (ie. 2nd cytosol sample), whereas another protein might have an **L:H** ratio of 2.2 but be considered non-significant if it was a member of a population with a positive mean $\log_2$L:H and a larger standard deviation (ie. 1st nuclear sample). Thus, although some studies have set **L:H** ratio significance levels ranging from as little as 1.4-fold (29) or less, to as much as 3-fold (49), we elected to assign significance based upon z-scores, with a few exceptions. Of the 4817 total identified proteins, only 128 were found exclusively in the nuclei fractions derived from

the preliminary limited 1D-SDS-PAGE/1D-LC analyses; thus, we focused further analyses on the 4689 cytosolic proteins, with the expectation that the nuclear proteins will be studied more extensively at a later date.

Using the above criteria, we identified and measured 127 proteins that were significantly up-regulated (Table 2). A protein was usually included in this table if a minimum of ½ of its biologic replicate z-scores were >1.960σ. Proteins were not considered significantly regulated if there were significant differences in their z-scores from the 2 technical replicates of the 3rd 2D-HPLC analysis. Some of the significantly up-regulated proteins included Vimentin and Mx2, known to be upregulated by inflammation and/or influenza virus infection, and both upregulated about 5 – 7-fold. Although the significance of each protein's fold-change was based upon z-score, we also include every protein's "average" fold-level alteration, determined by averaging each protein's $\log_2$L:H value from every observation (Supplementary Table T-1). A total of 153 proteins were significantly down-regulated using the same inclusion and exclusion criteria as above (Table 3). Many of these, including 38 (such as ARHGAP5, cyclophilin-33A, and the *Vav* 3 oncogene) were highly significantly down-regulated (z-score < -4.0σ), and down-regulated > 100-fold.

Validation of SILAC ratios by Western blotting

To confirm some of the SILAC-determined protein ratios, we analyzed selected proteins in infected and mock-infected cells by immunoblotting. Although there are a limited number of appropriate immunological reagents for most of the SILAC-measured proteins we identified in this study, we confirmed that Vimentin and β-2-microglobulin were up-regulated (Fig. 3). A number of proteins usually used as Western blot loading controls, such as GAPDH, which was found in every experiment at an **L:H** ratio of 1.1 ± 0.1, and Actin, with a measured average **L:H** ratio of 1.1, were present at equivalent levels in infected and mock-infected cells, as measured also by immunoblotting. Most other tested proteins were suggested by SILAC analysis to not be significantly regulated (**L:H** ratio 1.0 ± 0.3 and z-scores within

0.5σ of 0.0) and these relative levels were generally confirmed by Western blotting. Of note, 2 major Parp bands in Fig. 3 have M_r of 80 and 110kDa and immunoblots suggest they are slightly down-regulated 0.5- to 0.6-fold. The Parp protein was returned as a number of gi identifications, including gi|337424 and gi|22902366, which had **L:H** ratios of about 0.76 and z-scores of approximately -0.2. We also tested the quantity of keratins, many of which appeared to be highly significantly up-regulated in numerous SILAC experiments (**L:H** ratios > 5.0 and z-scores >3.0). However, immunoblotting indicated nearly equivalent amounts of cytokeratin 10 in infected and mock-infected cells. Thus, except for keratins, which are usually considered contaminants in MS experiments, immunoblotting validated the SILAC-determined values.

Proteins up-regulated by influenza virus infection are associated with responses to stimuli and protein binding, localization and transport, whereas down-regulated proteins are associated with alternative splicing, nucleotide and nucleoside activities, catabolic and hydrolase functions, and cell adhesion.

Proteins, and their levels of regulation, were analyzed by a variety of means. Protein gi numbers were imported into Uniprot (http://www.uniprot.org/) and converted into HUGO nomenclature committee (HGNC) identifiers. Several hundred gi numbers could not be mapped to HGNC ID numbers and several hundred gi numbers were collapsed to about ½ as many genes. This resulted in about 3900 unique HGNC IDs for the dataset (Supplementary Table T-1). Several of the different gi numbers that were collapsed into fewer genes may represent different isoforms of the same genes. The HGNC IDs that represented various sets of significantly up-regulated and down-regulated proteins at different confidence intervals of 95, 99, and 99.9% were then separately imported into DAVID (19,41), gene identifications converted to Entrez gene IDs by that suite of programs, and ontological functions determined by GOTERM, PANTHER and KEGG. We also analyzed the up-regulated proteins at each confidence interval after removing keratins from the datasets. Biological processes, functional annotations, molecular functions,

and cellular components identified at 95% confidence are depicted in Fig. 4 and data at all confidence levels are shown in Supplementary Table T-2.

Up-regulated proteins were assigned to 41 GOTERM biological processes at 95% confidence (Fig. 4A, left; Supplementary Table T-2), that included immune and defense responses, responses to stress and to virus, MHC-I mediated immunity pathways, and protein localization and transport. These up-regulated proteins were also assigned to 21 functional groups (Fig. 4B – including acetylation, cytoplasm, MHC-I and –II, phosphoprotein, and nucleotide binding), 19 cell component groups (Fig. 4C – including cytoplasm, Golgi, and organelle membranes), and 9 molecular functions (Fig. 4D – most notably nucleotide and ribonucleotide binding). PANTHER also assigned up-regulated proteins to mRNA transcription regulation, cell structure, molecular binding and MHC-I mediated immunity pathways (data not shown). Re-running the analysis after removing keratins led to the removal of blood coagulation and cytoskeletal groups from the above categories. Down-regulated proteins were assigned to 56 biological processes at 95% confidence (Fig. 4A, right; Supplementary Table T-2), that included localization determinants, transport, and positive regulation of apoptosis. These down-regulated proteins were also assigned to 28 functional groups, including acetylation, phosphoproteins, and alternative splicing (Fig. 4B), 27 cell component groups (Fig. 4C – including non-membrane-bounded organelles and adhesion-related components), and 28 molecular functions (Fig. 4D – including molecular binding and ATPase activity). PANTHER also assigned down-regulated proteins to MHC-II mediated immunity, nucleoside, nucleotide and nucleic acid metabolism, adhesion and cytoskeleton regulation. KEGG assigned proteins that had been down-regulated >100-fold to a number of cell pathways, including focal adhesion, cell adhesion and regulators of the actin cytoskeleton.

Protein gi numbers and levels of regulation were also imported into the Ingenuity Pathways Analysis (IPA®) tool and interacting pathways were constructed. A total of 18 pathways were identified at a confidence level of 95% or greater. Four of these pathways, each with 12 or more "focus" members (significantly up- or down-regulated proteins), shared common members (Fig. 5A) and it was possible to build a single, merged pathway (Fig. 5B). The other 14 pathways consisted of several proteins, but

contained only a single focus protein (data not shown). The 4 networks that contained 12 or more focus members corresponded to hair, skin and organ development, cell cycle, cell death, cancer, infection mechanisms, and antigen presentation pathways (Fig. 5C-F). Proteins present in the pathways and identified in our analyses as up-regulated are depicted in shades of red and include Mx1, LTF and VIM, proteins present in the pathways and identified as down-regulated are shown in green and include ERC1, L1CAM and CTNNB1, proteins present in the pathways and identified in our analyses, but neither up- nor down-regulated, are depicted in grey and include SMAD3, SCARB1 and RNA Pol II, and proteins known to participate in the pathways but not identified in our analyses are shown in white and include MYC, MAP3K1 and TP53. IPA analyses identify interaction nodes. For example, several of the highly up-regulated proteins interact with a few other proteins, but some, such as VIM and KHDRBS1 interact with four or more. Similarly, a few of the down-regulated proteins interact with few partners, but several, including CTNNB1, appear as interaction "hubs". We identified numerous other interaction hubs, such as SCARB1, CHUK, HSPB1, SMAD3, CTNND1, TIAL1, and SMAD2 which were not, themselves, significantly altered, but which interacted with several differentially regulated proteins.

Discussion

A number of studies have defined the cellular networks that are required or manipulated by influenza infection by use of genome wide RNAi screens, mRNA microarray screens and yeast 2-hybid assay, to identify 1449 protein targets for further analysis (73). Because viral infection leads to both qualitative and quantitative effects on host gene expression and function, we have complemented these previous studies by deriving a quantitative proteomic assessment of influenza infection to further define the effects of influenza virus infection on host functions. Whereas a variety of quantitative proteomic methods have been employed to examine perturbations in host protein quantities after virus infection, quantification of

host protein responses after influenza virus infection had only previously been reported after 2D-DIGE analysis, which identified 25 or fewer proteins (48,72). Here we present the application of SILAC and demonstrate several advantages relative to this earlier approach. While 2D-DIGE is excellent for resolving protein species that differ in post-translational modification, such as phosphorylation, it suffers several drawbacks, including a relatively low dynamic range and sample overloading (13), variability in labeling efficiency as well as labeling deficits for proteins lacking lysine or cysteine residues, and is unsuited for proteins at the extremes of molecular weight, alkalinity, or hydrophobicity (59). Finally, in-gel digestion methods are usually less efficient in allowing peptide identification than in-solution digestion which may partially explain why earlier studies identified less than 25 differentially-regulated proteins (48,72).

We used non-gel-based quantitative proteomic methods and identified and measured >120,000 SILAC-labeled peptides, which arose from >5000 host protein pairs. Almost 4700 cytosolic protein pairs were identified based upon stringent criteria that required 2 complete **L** and **H** tryptic peptides and protein identification confidence of 99% or greater. Of these, statistical tests indicated that 280 proteins (127 up-regulated and 153 down-regulated) were reliably identified as significantly regulated at the 95% confidence limit. Up-regulated proteins included those involved in stress responses, regulation of mRNA transcription, translation initiation, cell structure, molecular binding and MHC-I mediated immunity pathways. Down-regulated proteins include those involved in alternative splicing, MHC-II mediated immunity, nucleoside, nucleotide and nucleic acid metabolism, adhesion and cytoskeleton regulation. Several proteins (described in more detail below) had been previously described in other studies, but our application of SILAC in combination with multiple purification and fractionation schemes, identified more than 10 times as many differentially regulated proteins as have previously been identified in influenza virus infections.

A small number of host proteins have been reported as up-regulated by influenza virus infection in earlier quantitative proteomic studies. Keratins, including cytokeratin 10, have repeatedly been shown up-regulated as much as 50-fold by A/PR/8/34 infection (3-5,48,72). Alterations in these proteins would be

expected to have dramatic effects upon intermediate filaments and cellular organization, both of which play significant roles in enveloped virus intracellular transport and budding. However, keratins are also common contaminants in MS experiments and our Western blot assays suggest that this may have been the case in these studies, as the highly elevated **L:H** ratios could result from sample contamination with normal unlabeled keratins. This possibility could be tested in follow-up studies by infecting the **H**-labeled cells, which, if keratins are contaminants, would result in very low **L:H** ratios. A larger number of genes have been reported affected by influenza virus infection by microarray studies (6,30). We attempted to correlate our results with these previous transcriptomic analyses and found generally good correlation, as has also been reported in a transcriptomic/"semi-quantitative" proteomic comparison (6). Most of the 22 genes whose products we measured and for which transcriptomic data are readily available correlated well; only 3 were negatively correlated, such that micro-arrays indicated STAT3, SNX6 and VIM mRNA levels were up-regulated, not affected, and decreased (30), respectively, whereas SILAC indicated the corresponding proteins were slightly down-regulated, up-regulated, and highly up-regulated, respectively (data not shown).

The myxovirus resistance host proteins Mx1 and Mx2 have been identified as up-regulated by influenza infection in several studies, including microarray (30) and in more recent proteomic analyses (6,72). These interferon-induced, large GTPase dynamin-like Mx proteins are important anti-viral proteins, particularly against RNA viruses (37,38). "Semi-quantitative" analyses of macaque lungs infected by recombinant influenza virus A/Texas/36/91 (H1N1) suggested an approximate 3-fold up-regulation in this protein and quantitative 2-D DIGE of A549 cells infected with PR8 showed about 5- and 10-fold up-regulation at 48 and 72 hours post-infection (72). Although MxA (the mouse homolog of Mx1) was apparently not detected at 24hpi in A549 cells in the earlier study, these values are in good agreement with our measurements of ~5-14-fold increases in Mx proteins by PR8 infection in the current study. Vester et al (72) reported that nucleobindin was up-regulated approximately 2-fold by 72hpi, although it either was not detected, or was not up-regulated, at earlier time points in their study. Our results indicate nucleobindins were moderately affected, but not significantly at 24hpi (Supplementary

Table T-1). In addition, Vester et al reported proteasome activator hPA28 subunit β was also up-regulated about 2-fold by 72hpi, although it either was not detected, or was not up-regulated, at earlier time points in their study. Our results identified a larger number of proteasome-related molecules and indicated proteasome inhibitor subunit 1 isoform 1 was up-regulated about 2.2-fold, proteasome subunit α type 8 was down-regulated nearly 3-fold, and numerous other proteasome activators, including PA28β (up-regulated 1.2-fold) were only moderately altered at 24hpi. Reduction in specific host proteins may be mediated by enhanced proteasomal protein production and activity.

Our study identified many more up-regulated and down-regulated proteins. Notably, some of these have not been reported in previous quantitative influenza virus infections but have been reported as regulated by other viruses. For example, the intermediate filament protein vimentin, seen up-regulated to about 7-fold in our study (Table 2), has been reported increased by other (-)-sense RNA viruses, including rabies virus (76) and the (+)-sense RNA virus hepatitis C (50), but was reported down-regulated by West Nile virus (57), HIV (60), infectious bursal disease virus (79), and human papillomavirus type 16 (44). In addition, dermcidin, a sweat gland-produced antibiotic (51,63) that activates keratinocytes (54) and had been seen up-regulated by HIV infection (58), was also up-regulated almost 10-fold in our study, suggesting it may be activated by a broad range of infectious agents. Other notable innate immunity molecules that we found up-regulated include IFITM2, B2M, and the ISG15 ubiquitin-like modifier that is involved in IFN-induced inactivation of viral NS1 functions (78).

Most previous quantitative proteomic analyses identified very few influenza virus-induced down-regulated proteins. This might be expected because 2D-DIGE is generally limited to analysis of high-abundance proteins (13,59,72). This would not be a limitation if barely-detectable proteins are up-regulated above the detection threshold, but down-regulation of barely-detectable proteins below the detection limit might preclude their inclusion in the analyses. The down-regulated proteins we identified are involved in a very large number of cellular processes (Fig. 4), and include, most notably, those involved in MHC-II mediated immunity, protein folding and modification, nucleoside, nucleotide and

nucleic acid metabolism, adhesion and cytoskeleton regulation. Several notable proteins were detected and measured multiple times, and found significantly down-regulated. These include: β-catenin, found down-regulated ~3-fold, a key component of cell adhesion pathways and a target for the ubiquitin proteasome pathway (reviewed in (1)) that also is involved in regulating lung development (17). Down regulation of the β-catenin protein may avoid IFN induction through the WNT/β-catenin pathway (64). In addition, the WD40 protein, that is involved in signal transduction, molecular binding, particularly with β-catenin, and numerous other processes, and that is targeted by retroviral insertion (42) and required to aid herpesvirus replication (66), was found down-regulated ~100-fold in our study.

Influenza infection is critically dependent on host gene expression because there is a strict requirement for host POL II transcripts as a source of capped oligonucleotides for priming viral transcription, as well as a requirement for splicing machinery to generate NEP and M2 spliced transcripts (reviewed in (24)). Therefore, influenza virus must maintain and regulate host transcriptional activities to optimize viral replication, via the enhanced production of canonical transcription factors such as TFIIB, TFIIF1 and TFIID7, while down-regulating most of the other typical POL II transcription factors. Thus influenza virus may modulate expression of host POL II transcripts to favor viral replication processes, such as the association of influenza polymerase with POL II early in transcription that may be involved in accessing newly formed capped transcripts as they are produced and concomitantly inhibiting elongation (10,25). The general transcription factor TFIIA, that regulates RNA POL2-dependent DNA transcription (40), was down-regulated ~4-fold. This protein would not be expected to be needed by an RNA virus that uses no DNA intermediates in its replication; however, down-regulation of host DNA dependent transcription would be important for host resistance genes such as IFN and IFN inducible genes (36). TACC2 (transforming, acidic coiled-coil containing protein 2 isoform-a), a centrosomal-microtubule-associated protein (31) involved in protein translation and RNA processing and transcription (68) was found down-regulated >12-fold. Interestingly, this protein is targeted for degradation by SV40 virus (70), suggesting disparate viruses may benefit from targeting this host protein.

On the other hand, influenza virus has mechanisms for down regulation of gene expression that involve inhibition of polyadenylation through binding of NS1-viral polymerase complexes to cleavage and polyadenylation specific factor 30 (47) that serves to block host gene expression. This blocks the expression of host inhibitors including interferon and TNFα (that were reduced in PR8 infected A549 cells (Table 3), and thus a balance of host inhibition must be achieved while maintaining host gene transcription of mRNA and protein products employed for replication. Influenza NS1 protein also binds eIF4G1 and PABP1 translation initiation factors to favor influenza protein translation (9,18,69) relative to host translation. It is possible that the reduction in eIF4G1 as well as many ribosomal protein components may be involved in the mechanisms for preferential viral gene expression at the expense of host gene expression.

Influenza infection also enhances immune evasion by directing the incorporation of MHC-I into ganglioside rich microdomains that function to recruit cellular inhibitors of NK cell binding and function (reviewed in (14)) which is consistent with an up-regulation of MHC-I in A549 cells (Table 2; Fig. 4). The down regulation of several components of the MHC-I antigen presentation machinery would also be expected to reduce influenza antigen presentation on the surface of infected cells to result in immune cell mediated attack. The up-regulation of ubiquitin activities as well as the IFN-induced viral antagonist, Mx1, may be an interrelated feature of Mx1 control because Mx1 is found in nuclear PML bodies in infected cells that are also sites of ubiquitin degradation (26). We found Mx1 up-regulated 14-fold (z-score >5) in our nuclear fractions, which, as explained earlier, was not further analyzed in the present study (data not shown). With respect to the cytoskeleton components, influenza virus uses actin interactions of NP protein for nucleocytoplasmic transport of RNP (21,65) and the multiple instances of increases in actins and related components may be instrumental in favoring viral replication. Other up-regulated proteins listed in Table 2 and down-regulated proteins listed in Table 3 could be hypothesized to have been affected by infection but will not be discussed further at this time, as they await further validation.

In summary, we have applied SILAC to quantitatively measure the regulation of nearly 4700 host cytosolic proteins after human A549 lung cells were infected with prototype influenza lab strain A/PR/8/34. Most proteins measured by this non-biased approach were not substantially altered, having **L:H** ratios of approximately 1.0. We chose a relatively rigorous statistical cut-off by requiring proteins' z-score values to be >1.96 standard deviation units away from population means, corresponding to 95% confidence. Our study approach was unbiased with respect to any particular groups of proteins because we made no attempt to enrich for any subpopulation of proteins or specific modifications. This study could be extended by analyzing, for example, nuclei of infected cells or phosphorylated proteins. It also will be important to extend these types of analyses to other cell types, including primary airway cells and to other virus types, including more clinically relevant strains, such as the current pandemic H1N1 2009 influenza virus. These types of analyses should identify common, as well as unique, features of each virus-host interaction and may point the way to better designed anti-viral therapies.

Acknowledgements

This work was supported by grants MT-11630 and PAN-83159 from the Canadian Institutes of Health Research to K.M.C. The authors thank Kolawole Opanubi for expert technical assistance, Dr. James House, Director, Animal Sciences for embryonated hens eggs in which some influenza virus stocks were grown, Dr. Ming Yang for anti-influenza virus NP monoclonal hybridoma cells, and Dr. Yoshihiro Kawaoka for the influenza virus reverse genetics system.

Contributions

K.M.C., D.K., J.A.W., and E.G.B. designed experiments, K.M.C., A.B., W.X., X.M., and D.K. performed experimental work described herein, O.K. performed mass spectrometry, J.P.C performed database and computational analyses, and all co-authors edited the manuscript.

Conflicts of Interest

The authors declare no conflicts of interest.

Figure Legends

Figure 1. Photomicrographs of A549 cells infected with A/PR/8/34 at MOI = 7 PFU/cell (bottom), or mock-infected (top) for the indicated hours post-infection (indicated at top). Scale bar = 100μm.

Figure 2. Distributions of proteins identified in various experiments. **A.** and **B.** Venn diagrams of numbers of identified proteins from various analyses. **A.** Proteins from A/PR/9/34-infected A549 cells were fractionated into the cytosolic + crude membrane (Cyto/Gel) and nuclei (Nuclei/Gel) fractions and resolved in SDS-PAGE, then subjected to tryptic digest before 1-D LC/MS. Alternatively, proteins were harvested from cytosolic and crude membrane fractions, digested with trypsin, then peptides resolved by 2-D orthogonal LC/MS (2D-LC/MS). Results compiled from 2 replicate experiments. **B.** Proteins identified by the three separate 2D-LC/MS analyses. Proteins from the 2 technical replicate analyses of the third 2D-LC/MS run were merged prior to being combined with other data. **C.** Frequency distributions of identified proteins in two Influenza virus-infected A549 sample sets, with **L:H** ratios expressed as Log_2 values. Positive values represent up-regulated host proteins in virus-infected cells; negative values represent down-regulated host proteins. Only the distributions of one SDS-PAGE analysis and one 2D-LC/MS analysis are shown for clarity. Note that distributions are not identical, with different peak breadth, and not perfectly normal, with the 2D-LC/MS sample exhibiting several substantially down-regulated proteins at ~ $-13log_2$. Characteristics of all SDS-PAGE and 2D-LC/MS protein distributions, mean log_2L:H ratios and standard deviations of log_2L:H ratios are shown in Table 1.

Figure 3. Immunoblot analysis of host and influenza virus proteins in mock-infected (M) and Influenza virus strain A/PR/8/34 (H1N1)-infected (I) A549 cells. Cells were harvested and lysed with 0.5% NP-40

detergent, nuclei removed, and cytosolic fractions dissolved in SDS electrophoresis sample buffer, resolved in 5-15% mini gradient SDS-PAGE, transferred to PVDF, and probed with various antibodies. Bands were visualized, and intensities measured, with an Alpha Innotech FluorChem®Q MultiImage® III instrument. Molecular weight standards are indicated at left and ratios of each protein (infected divided by mock-infected) are indicated for each protein at right, along with SILAC-measured ratios (far right). *: No viral proteins measured by SILAC because not present in mock-infected samples.

Figure 4. Gene ontology analyses of up-regulated and down-regulated proteins. The proteins identified in Tables 2 and 3, as well as non-keratin proteins in Table 2, were imported into the DAVID gene ontology suite of programs at the NIAID, gene identifications converted by that program, and ontological functions determined by GOTERM. **A**, Biological processes; **B**, Functional annotations; **C**, Cellular components; and **D**, Molecular functions, and the numbers of identified genes associated with each group, identified at a confidence level of 95% are illustrated. *: Processes, functions and cellular components that are removed when keratins excluded from input gene list. Additional lists of functional groups, processes and components at different confidence limits are indicated in Supplementary Table T-2.

Figure 5. Molecular pathways of regulated proteins. Proteins and their levels of regulation, were imported into the Ingenuity Pathways Analysis (IPA®) tool and interacting pathways were constructed. **A.** Overview of 4 networks identified at 95% confidence and each of which contained 10 or more "focus" molecules (molecules significantly up- or down-regulated). Each box contains arbitrary network number (upper) as well as number of focus molecules within the network (lower bolded number). Lines connecting networks indicate number of focus molecules present in each attached network. **B.** Merged network, containing all molecules present in each of the four individual networks. **C. – F.** Individual networks with pathway names indicated. Solid lines: direct known interactions; dashed lines: suspected or indirect interactions; red: significantly up-regulated proteins; pink: moderately up-regulated proteins; grey: proteins identified but not significantly regulated; light green: moderately down-regulated proteins;

dark green: significantly down-regulated proteins; white: proteins known to be in network, but not identified in our study. Molecular classes are indicated in legend.

References

1. **Aberle, H., A. Bauer, J. Stappert, A. Kispert, and R. Kemler**. 1997. beta-catenin is a target for the ubiquitin-proteasome pathway. EMBO J. **16**:3797-3804.
2. **Alexander, D. J.** 2007. An overview of the epidemiology of avian influenza. Vaccine **25**:5637-5644.
3. **Arcangeletti, M. C., F. De Conto, F. Ferraglia, F. Pinardi, R. Gatti, G. Orlandini, S. Covan, F. Motta, I. Rodighiero, G. Dettori, and C. Chezzi**. 2008. Host-cell-dependent role of actin cytoskeleton during the replication of a human strain of influenza A virus. Arch. Virol. **153**:1209-1221.
4. **Arcangeletti, M. C., F. Pinardi, S. Missorini, F. DeConto, G. Conti, P. Portincasa, K. Scherrer, and C. Chezzi**. 1997. Modification of cytoskeleton and prosome networks in relation to protein synthesis in influenza A virus-infected LLC-MK2 cells. Virus Res. **51**:19-34.
5. **Avalos, R. T., Z. Yu, and D. P. Nayak**. 1997. Association of influenza virus NP and M1 proteins with cellular cytoskeletal elements in influenza virus-infected cells. J. Virol. **71**:2947-2958.
6. **Baas, T., C. R. Baskin, D. L. Diamond, A. Garcia-Sastre, H. Bielefeldt-Ohmann, T. M. Tumpey, M. J. Thomas, V. S. Carter, T. H. Teal, N. Van Hoeven, S. Proll, J. M. Jacobs, Z. R. Caldwelll, M. A. Gritsenko, R. R. Hukkanen, D. G. Camp, R. D. Smith, and M. G. Katze**. 2006. Integrated molecular signature of disease: Analysis of influenza virus-infected macaques through functional genomics and proteomics. J. Virol. **80**:10813-10828.
7. **Bonaldi, T., T. Straub, J. Cox, C. Kumar, P. B. Becker, and M. Mann**. 2008. Combined use of RNAi and quantitative proteomics to study gene function in Drosophila. Mol. Cell **31**:762-772.
8. **Brown, E. G.** 1990. Increased virulence of a mouse-adapted variant of Influenza A/Fm/1/47 virus is controlled by mutations in genome segments 4, 5, 7, and 8. J. Virol. **64**:4523-4533.
9. **Burgui, I., T. Aragon, J. Ortin, and A. Nieto**. 2003. PABP1 and eIF4Gl associate with influenza virus NS1 protein in viral mRNA translation initiation complexes. J. Gen. Virol. **84**:3263-3274.
10. **Chan, A. Y., F. T. Vreede, M. Smith, O. G. Engelhardt, and E. Fodor**. 2006. Influenza virus inhibits RNA polymerase II elongation. Virology **351**:210-217.
11. **Chen, R., S. Pan, R. Aebersold, and T. A. Brentnall**. 2007. Proteomics studies of pancreatic cancer. Proteomics Clin. App. **1**:1582-1591.
12. **Choe, L. H., K. Aggarwal, Z. Franck, and K. H. Lee**. 2005. A comparison of the consistency of proteome quantitation using two-dimensional electrophoresis and shotgun isobaric tagging in Escherichia coli cells. Electrophoresis **26**:2437-2449.
13. **Corthals, G. L., V. C. Wasinger, D. F. Hochstrasser, and J. C. Sanchez**. 2000. The dynamic range of protein expression: A challenge for proteomic research. Electrophoresis **21**:1104-1115.
14. **Culley, F. J.** 2009. Natural killer cells in infection and inflammation of the lung. Immunology **128**:151-163.

15. **de Godoy, L. M. F., J. V. Olsen, J. Cox, M. L. Nielsen, N. C. Hubner, F. Frohlich, T. C. Walther, and M. Mann**. 2008. Comprehensive mass-spectrometry-based proteome quantification of haploid versus diploid yeast. Nature **455**:1251-1U60.
16. **de Hoog, C. L., L. J. Foster, and M. Mann**. 2004. RNA and RNA binding proteins participate in early stages of cell spreading through spreading initiation centers. Cell **117**:649-662.
17. **De Langhe, S. P., G. Carraro, D. Tefft, C. G. Li, X. Xu, Y. Chai, P. Minoo, M. K. Hajihosseini, J. Drouin, V. Kaartinen, and S. Bellusci**. 2008. Formation and differentiation of multiple mesenchymal lineages during lung development is regulated by beta-catenin signaling. PLoS ONE **3**:e1516-PMID18231602.
18. **Delaluna, S., P. Fortes, A. Beloso, and J. Ortin**. 1995. Influenza-virus NS1 protein enhances the rate of translation initiation of viral messenger-RNAs. J. Virol. **69**:2427-2433.
19. **Dennis, G., B. T. Sherman, D. A. Hosack, J. Yang, W. Gao, H. C. Lane, and R. A. Lempicki**. 2003. DAVID: Database for annotation, visualization, and integrated discovery. Genome Biology **4**.
20. **DeSouza, L., G. Diehl, M. J. Rodrigues, J. Z. Guo, A. D. Romaschin, T. J. Colgan, and K. W. M. Siu**. 2005. Search for cancer markers from endometrial tissues using differentially labeled tags iTRAQ and clCAT with multidimensional liquid chromatography and tandem mass spectrometry. J. Proteome Res. **4**:377-386.
21. **Digard, P., D. Elton, K. Bishop, E. Medcalf, A. Weeds, and B. Pope**. 1999. Modulation of nuclear localization of the influenza virus nucleoprotein through interaction with actin filaments. J. Virol. **73**:2222-2231.
22. **Dwivedi, R. C., V. Spicer, M. Harder, M. Antonovici, W. Ens, K. G. Standing, J. A. Wilkins, and O. V. Krokhin**. 2008. Practical implementation of 2D HPLC scheme with accurate peptide retention prediction in both dimensions for high-throughput bottom-up proteomics. Anal. Chem. **80**:7036-7042.
23. **Elliott, M. H., D. S. Smith, C. E. Parker, and C. Borchers**. 2009. Current trends in quantitative proteomics. J. Mass Spectrom. **44**:1637-1660.
24. **Engelhardt, O. G. and E. Fodor**. 2006. Functional association between viral and cellular transcription during influenza virus infection. Rev. Med. Virol. **16**:329-345.
25. **Engelhardt, O. G., M. Smith, and E. Fodor**. 2005. Association of the influenza a virus RNA-dependent RNA polymerase with cellular RNA polymerase II. J. Virol. **79**:5812-5818.
26. **Engelhardt, O. G., E. Ullrich, G. Kochs, and O. Haller**. 2001. Interferon-induced antiviral Mx1 GTPase is associated with components of the SUMO-1 system and promyelocytic leukemia protein nuclear bodies. Exp. Cell Res. **271**:286-295.
27. **Everley, P. A., J. Krijgsveld, B. R. Zetter, and S. P. Gygi**. 2004. Quantitative cancer proteomics: Stable isotope labeling with amino acids in cell culture (SILAC) as a tool for prostate cancer research. Mol. Cell Proteomics. **3**:729-735.
28. **Feinberg, A. P.** 2007. Phenotypic plasticity and the epigenetics of human disease. Nature **447**:433-440.
29. **Garcia-Ramirez, M., F. Canals, C. Hernandez, N. Colome, C. Ferrer, E. Carrasco, J. Garcia-Arumi, and R. Simo**. 2007. Proteomic analysis of human vitreous fluid by fluorescence-based difference gel electrophoresis (DIGE): a new strategy for identifying potential candidates in the pathogenesis of proliferative diabetic retinopathy. Diabetologia **50**:1294-1303.
30. **Geiss, G. K., M. Salvatore, T. M. Tumpey, V. S. Carter, X. Y. Wang, C. F. Basler, J. K. Taubenberger, R. E. Bumgarner, P. Palese, M. G. Katze, and A. Garcia-Sastre**. 2002. Cellular

transcriptional profiling in influenza A virus-infected lung epithelial cells: The role of the nonstructural NS1 protein in the evasion of the host innate defense and its potential contribution to pandemic influenza. Proc. Natl. Acad. Sci. U. S. A **99**:10736-10741.

31. **Gergely, F., C. Karlsson, I. Still, J. Cowell, J. Kilmartin, and J. W. Raff**. 2000. The TACC domain identifies a family of centrosomal proteins that can interact with microtubules. Proc. Natl. Acad. Sci. U. S. A **97**:14352-14357.
32. **Gilar, M., P. Olivova, A. E. Daly, and J. C. Gebler**. 2005. Orthogonality of separation in two-dimensional liquid chromatography. Analytical Chemistry **77**:6426-6434.
33. **Goldberg, A. D., C. D. Allis, and E. Bernstein**. 2007. Epigenetics: A landscape takes shape. Cell **128**:635-638.
34. **Graumann, J., N. C. Hubner, J. B. Kim, K. Ko, M. Moser, C. Kumar, J. Cox, H. Scholer, and M. Mann**. 2008. Stable isotope labeling by amino acids in cell culture (SILAC) and proteome quantitation of mouse embryonic stem cells to a depth of 5,111 proteins. Mol. Cell Proteomics. **7**:672-683.
35. **Gygi, S. P., B. Rist, S. A. Gerber, F. Turecek, M. H. Gelb, and R. Aebersold**. 1999. Quantitative analysis of complex protein mixtures using isotope-coded affinity tags. Nat. Biotechnol. **17**:994-999.
36. **Hale, B. G., R. E. Randall, J. Ortin, and D. Jackson**. 2008. The multifunctional NS1 protein of influenza A viruses. J. Gen. Virol. **89**:2359-2376.
37. **Haller, O. and G. Kochs**. 2002. Interferon-induced mx proteins: Dynamin-like GTPases with antiviral activity. Traffic **3**:710-717.
38. **Haller, O., P. Staeheli, and G. Kochs**. 2009. Protective role of interferon-induced Mx GTPases against influenza viruses. Rev. Sci. Tech. **28**:219-231.
39. **Han, D. K., J. Eng, H. L. Zhou, and R. Aebersold**. 2001. Quantitative profiling of differentiation-induced microsomal proteins using isotope-coded affinity tags and mass spectrometry. Nature Biotech. **19**:946-951.
40. **Hoiby, T., H. Q. Zhou, D. J. Mitsiou, and H. G. Stunnenberg**. 2007. A facelift for the general transcription factor TFIIA. Biochim. Biophys. Acta-Gene Struct. Exp. **1769**:429-436.
41. **Huang, D. W., B. T. Sherman, and R. A. Lempicki**. 2009. Systematic and integrative analysis of large gene lists using DAVID bioinformatics resources. Nature Protocols **4**:44-57.
42. **Jiang, X. Y., Z. Hanna, M. Kaouass, L. Girard, and P. Jolicoeur**. 2002. Ahi-1, a novel gene encoding a modular protein with WD40-repeat and SH3 domains, is targeted by the Ahi-1 and Mis-2 provirus integrations. J. Virol. **76**:9046-9059.
43. **Keshamouni, V. G., P. Jagtap, G. Michailidis, J. R. Strahler, R. Kuick, A. K. Reka, P. Papoulias, R. Krishnapuram, A. Srirangam, T. J. Standiford, P. C. Andrews, and G. S. Omenn**. 2009. Temporal quantitative proteomics by iTRAQ 2D-LC-MS/MS and corresponding mRNA expression analysis identify post-transcriptional modulation of actin-cytoskeleton regulators during TGF-beta-induced epithelial-mesenchymal transition. J. Proteome Res. **8**:35-47.
44. **Kim, E., J. Kang, M. Cho, S. Lee, E. Seo, H. Choi, Y. Kim, J. Kim, K. Y. Kang, K. P. Kim, J. Han, Y. Sheen, Y. N. Yum, S. N. Park, and D. Y. Yoon**. 2009. Profiling of transcripts and proteins modulated by the E7 oncogene in the lung tissue of E7-Tg mice by the omics approach. Mol. Med. Rep. **2**:129-137.
45. **Kobasa, D., S. M. Jones, K. Shinya, J. C. Kash, J. Copps, H. Ebihara, Y. Hatta, J. H. Kim, P. Halfmann, M. Hatta, F. Feldmann, J. B. Alimonti, L. Fernando, Y. Li, M. G. Katze, H.**

Feldmann, and Y. Kawaoka. 2007. Aberrant innate immune response in lethal infection of macaques with the 1918 influenza virus. Nature **445**:319-323.

46. **Krauss, S., C. A. Obert, J. Franks, D. Walker, K. Jones, P. Seiler, L. Niles, S. P. Pryor, J. C. Obenauer, C. W. Naeve, L. Widjaja, R. J. Webby, and R. G. Webster**. 2007. Influenza in migratory birds and evidence of limited intercontinental virus exchange. Plos Pathogens **3**:1684-1693.
47. **Kuo, R. L. and R. M. Krug**. 2009. Influenza A virus polymerase is an integral component of the CPSF30-NS1A protein complex in infected cells. J. Virol. **83**:1611-1616.
48. **Liu, N., W. J. Song, P. Wang, K. C. Lee, W. Chan, H. L. Chen, and Z. W. Cai**. 2008. Proteomics analysis of differential expression of cellular proteins in response to avian H9N2 virus infection in human cells. Proteomics **8**:1851-1858.
49. **Lucitt, M. B., T. S. Price, A. Pizarro, W. Wu, A. K. Yocum, C. Seiler, M. A. Pack, I. A. Blair, G. A. FitzGerald, and T. Grosser**. 2008. Analysis of the zebrafish proteome during embryonic development. Mol. Cell Proteomics. **7**:981-994.
50. **Matos, J. M., F. A. Witzmann, O. W. Cummings, and C. M. Schmidt**. 2009. A pilot study of proteomic profiles of human hepatocellular carcinoma in the United States. J. Surg. Res. **155**:237-243.
51. **Murakami, M., T. Ohtake, R. A. Dorschner, B. Schittek, C. Garbe, and R. L. Gallo**. 2002. Cathelicidin anti-microbial peptide expression in sweat, an innate defense system for the skin. J. Invest. Dermatol. **119**:1090-1095.
52. **Nesvizhskii, A. I. and R. Aebersold**. 2005. Interpretation of shotgun proteomic data - The protein inference problem. Mol. Cell Proteomics. **4**:1419-1440.
53. **Neumann, G., T. Watanabe, H. Ito, S. Watanabe, H. Goto, P. Gao, M. Hughes, D. R. Perez, R. Donis, E. Hoffmann, G. Hobom, and Y. Kawaoka**. 1999. Generation of influenza A viruses entirely from cloned cDNAs. Proc. Natl. Acad. Sci. U. S. A **96**:9345-9350.
54. **Niyonsaba, F., A. Suzuki, H. Ushio, I. Nagaoka, H. Ogawa, and K. Okumura**. 2009. The human antimicrobial peptide dermcidin activates normal human keratinocytes. Brit. J. Dermatol. **160**:243-249.
55. **Ong, S. E. and M. Mann**. 2005. Mass spectrometry-based proteomics turns quantitative. Nature Cell Biol. **1**:252-262.
56. **Palese, P. and M. L. Shaw**. 2007. Orthomyxoviridae: The viruses and their replication, p. 1647-1689. *In* D. M. Knipe and P. M. Howley (eds.), Fields Virology. Lippincott Williams & Wilkins, Philadelphia.
57. **Pastorino, B., E. Boucomont-Chapeaublanc, C. N. Peyrefitte, M. Belghazi, T. Fusai, C. Rogier, H. J. Tolou, and L. Almeras**. 2009. Identification of cellular proteome modifications in response to West Nile virus infection. Mol. Cell Proteomics. **8**:1623-1637.
58. **Pathak, S., G. A. De Souza, T. Salte, H. G. Wiker, and B. Asjo**. 2009. HIV induces both a down-regulation of IRAK-4 that impairs TLR signalling and an up-regulation of the antibiotic peptide dermcidin in monocytic cells. Scand. J. Immunol. **70**:264-276.
59. **Patton, W. F.** 2002. Detection technologies in proteome analysis. J. Chromatogr. B-Anal. Technol. Biomed. Life Sci. **771**:3-31.
60. **Pocernich, C. B., D. Boyd-Kimball, H. F. Poon, V. Thongboonkerd, B. C. Lynn, J. B. Klein, V. Calebrese, A. Nath, and D. A. Butterfield**. 2005. Proteomics analysis of human astrocytes expressing the HIV protein Tat. Mol. Brain Res. **133**:307-316.

61. **Prange, A. and D. Proefrock**. 2008. Chemical labels and natural element tags for the quantitative analysis of bio-molecules. J. Anal. Atomic Spectrom. **23**:432-459.

62. **Prokhorova, T. A., K. T. G. Rigbolt, P. T. Johansen, J. Henningsen, I. Kratchmarova, M. Kassem, and B. Blagoev**. 2009. Stable isotope labeling by amino acids in cell culture (SILAC) and quantitative comparison of the membrane proteomes of self-renewing and differentiating human embryonic stem cells. Mol. Cell Proteomics. **8**:959-970.

63. **Schittek, B., R. Hipfel, B. Sauer, J. Bauer, H. Kalbacher, S. Stevanovic, M. Schirle, K. Schroeder, N. Blin, F. Meier, G. Rassner, and C. Garbe**. 2001. Dermcidin: a novel human antibiotic peptide secreted by sweat glands. Nature Immunology **2**:1133-1137.

64. **Shapira, S. D., I. Gat-Viks, B. O. V. Shum, A. Dricot, M. M. de Grace, L. G. Wu, P. B. Gupta, T. Hao, S. J. Silver, D. E. Root, D. E. Hill, A. Regev, and N. Hacohen**. 2009. A physical and regulatory map of host-influenza interactions reveals pathways in H1N1 infection. Cell **139**:1255-1267.

65. **Simpson-Holley, M., D. Ellis, D. Fisher, D. Elton, J. McCauley, and P. Digard**. 2002. A functional link between the actin cytoskeleton and lipid rafts during budding of filamentous influenza virions. Virology **301**:212-225.

66. **Smith, C. C., J. Nelson, L. Aurelian, M. Gober, and B. B. Goswami**. 2000. Ras-GAP binding and phosphorylation by herpes simplex virus type 2 RR1 PK (ICP10) and activation of the Ras/MEK/MAPK mitogenic pathway are required for timely onset of virus growth. J. Virol. **74**:10417-10429.

67. **Spicer, V., A. Yamchuk, J. Cortens, S. Sousa, W. Ens, K. G. Standing, J. A. Wilkins, and O. Krokhin**. 2007. Sequence-specific retention calculator. A family of peptide retention time prediction algorithms in reversed-phase HPLC: applicability to various chromatographic conditions and columns. Anal. Chem. **79**:8762-8768.

68. **Still, I. H., A. K. Vettaikkorumakankauv, A. DiMatteo, and P. Liang**. 2004. Structure-function evolution of the Transforming acidic coiled coil genes revealed by analysis of phylogenetically diverse organisms. BMC Evol. Biol. **4**.

69. **Taubenberger, J. K.** 2003. Fixed and frozen flu: the 1918 influenza and lessons for the future. Avian Dis. **47**:789-791.

70. **Tei, S., N. Saitoh, T. Funahara, S. Iida, Y. Nakatsu, K. Kinoshita, Y. Kinoshita, H. Saya, and M. Nakao**. 2009. Simian virus 40 large T antigen targets the microtubule-stabilizing protein TACC2. J. Cell Sci. **122**:3190-3198.

71. **Tian, Q., S. B. Stepaniants, M. Mao, L. Weng, M. C. Feetham, M. J. Doyle, E. C. Yi, H. Y. Dai, V. Thorsson, J. Eng, D. Goodlett, J. P. Berger, B. Gunter, P. S. Linseley, R. B. Stoughton, R. Aebersold, S. J. Collins, W. A. Hanlon, and L. E. Hood**. 2004. Integrated genomic and proteomic analyses of gene expression in mammalian cells. Mol. Cell Proteomics. **3**:960-969.

72. **Vester, D., E. Rapp, D. Gade, Y. Genzel, and U. Reichl**. 2009. Quantitative analysis of cellular proteome alterations in human influenza A virus-infected mammalian cell lines. Proteomics **9**:3316-3327.

73. **Watanabe, T., S. Watanabe, and Y. Kawaoka**. 2010. Cellular networks involved in the Influenza virus life cycle. Cell Host & Microbe **7**:427-439.

74. **Yang, M., Y. Berhane, T. Salo, M. Li, K. Hole, and A. Clavijo**. 2008. Development and application of monoclonal antibodies against avian influenza virus nucleoprotein. J. Virol. Meth. **147**:265-274.

75. **Yates, J. R., C. I. Ruse, and A. Nakorchevsky**. 2009. Proteomics by mass spectrometry: approaches, advances, and applications. Annu. Rev. Biomed. Eng. **11**:49-79.

76. **Zandi, F., N. Eslami, M. Soheili, A. Fayaz, A. Gholami, and B. Vaziri**. 2009. Proteomics analysis of BHK-21 cells infected with a fixed strain of rabies virus. Proteomics **9**:2399-2407.

77. **Zhang, Y., A. Wolf-Yadlin, P. L. Ross, D. J. Pappin, J. Rush, D. A. Lauffenburger, and F. M. White**. 2005. Time-resolved mass spectrometry of tyrosine phosphorylation sites in the epidermal growth factor receptor signaling network reveals dynamic modules. Mol. Cell Proteomics. **4**:1240-1250.

78. **Zhao, C., T. Y. Hsiang, R. L. Kuo, and R. M. Krug**. 2010. ISG15 conjugation system targets the viral NS1 protein in influenza A virus-infected cells. Proc. Natl. Acad. Sci. U. S. A **107**:2253-2258.

79. **Zheng, X. J., L. L. Hong, L. X. Shi, J. Q. Guo, Z. Sun, and J. Y. Zhou**. 2008. Proteomics analysis of host cells infected with infectious bursal disease virus. Mol. Cell Proteomics. **7**:612-625.

Table 1. Number of proteins, log_2L:H ratio means and standard deviations, and Z-scores of SILAC-labeled proteins identified by various purification schemes

Purification method Expt	# Prot	Mean Log_2L:H	STD Log_2	Z-scores ± 1.960σ (95%)	Z-scores ± 2.576σ (99%)	Z-scores ± 3.291σ (99.9%)
SDS-PAGE / LC						
1 Cytosol	248	0.029	0.565	8, 6[1]	8, 4	8, 1
Crude Membranes	273	0.085	0.531	9, 5	8, 3	8, 2
Nuclear	262	0.083	0.678	15, 1	14, 0	11, 0
2 Cytosol	467	-0.034	0.478	20, 9	9, 6	4, 4
Crude Membranes	524	0.011	0.422	22, 10	14, 8	11, 2
Nuclear	478	0.003	0.415	18, 12	13, 3	10, 2
2D-HPLC						
1	1890	0.013	0.633	44, 52	25, 35	20, 23
2	846	0.046	0.506	22, 15	17, 9	14, 5
3 Technical (1)	2509	-0.030	0.539	47, 67	33, 42	23, 30
Technical (2)	2574	-0.020	0.533	55, 65	35, 37	26, 29
Combined	3173	-0.025	0.537			

[1] First value is number of up-regulated proteins outside the indicated confidence level; second number is number of down-regulated proteins outside the indicated confidence level.

Table 2. A549 proteins increased > 95% confidence[1]

Accession	HGNC ID	Name	L:H Ratio[3]	Biol. Reps.	Z Score				
					2D-HPLC/MS[2]				SDS-PAGE[4]
					A	B	2DLC1	2DLC2	
Proteins measured in more than 1 biologic replicate									
gi|4755085	COL1A1	pro alpha 1(I) collagen	17.307	2					**5.845**
gi|6013427	ALBU	serum albumin precursor	9.979	2			**6.104**		**3.948**
gi|5031841	KRT6B	keratin 6B	8.514	3					**6.448**
gi|547749	K1C10	Keratin, type I cytoskeletal 10 (Cytokeratin-10) (CK-10) (Keratin-10) (K10)	7.214	7	**6.069**	**11.870**			**6.434**
gi|5030431	VIME	vimentin	6.944	2			**3.664**	**6.347**	
gi|5031839	K2C6A	keratin 6A	5.939	3	**4.559**				**3.044**
gi|55956899	K1C9	keratin 9	5.700	7			**5.481**		**5.888**
gi|17318569	KRT1	keratin 1	5.141	8	**8.213**	**12.290**	**2.308**		**5.600**
gi|49456703	Q6FH82	IFITM2	5.002	2					**6.397**
gi|2996631	Q75MY7	MX2	4.968	2			**4.771**		**3.406**
gi|56757580	K2C5	Keratin, type II cytoskeletal 5 (Cytokeratin-5) (CK-5) (Keratin-5) (K5) (58 kDa cytokeratin)	4.273	2					**4.445**
gi|47132620	K22E	keratin 2	4.243	7		**5.140**			**5.913**
gi|15431310	K1C14	keratin 14	3.762	4					**8.348**
gi|48146249	B2M	Beta-2-microglobulin	2.788	2					**3.775**
gi|14550514	UCRP	ISG15 ubiquitin-like modifier	2.735	3					**6.499**
gi|4580013	SNX6	sorting nexin-6, TRAF4-associated factor 2	2.608	2	-0.557			**6.024**	
gi|55960992	H2A2C	histone 2, H2ac	2.495	2				**4.848**	**0.098**
gi|55961043	SF13A	FUS interacting protein (serine-arginine rich) 1	2.293	2			**2.575**		**1.807**
gi|13279173	CSN4	COP9 constitutive photomorphogenic homolog subunit 4 (Arabidopsis)	2.287	2	0.040			**4.640**	
gi|34784772	GPI	glucose-6-phosphate isomerase	2.118	3			**6.172**		**-0.602**
gi|34783347	RAB15	RAB15, member RAS onocogene family	1.959	3		**5.252**			**0.148**
gi|56122599	Q5Q9Z3	leukemia multidrug resistance associated protein	1.865	2					**2.225**
gi|7705893	DCTN4	dynactin 4 (p62)	1.864	2	**2.884**	**4.081**	-0.086		
gi|4218955	FLNC	gamma-filamin	1.847	2		-0.325		**3.784**	
gi|13623669	HEXI1	Hexamethylene bis-acetamide inducible 1	1.746	2	**2.313**	**2.035**		0.833	

gi|39645500	SCYL2	SCY1-like 2 (S. cerevisiae)	1.699	2		**2.414**	0.396		
gi|40850903	Q549N5	Signal recognition particle receptor, B subunit	1.613	2	**2.626**	**2.207**	0.151		
gi|49457320	Q6FGE5	S100A10	1.567	6				0.324	**2.112**
gi|6031192	MPCP	solute carrier family 25 member 3 isoform a precursor	1.538	3			**3.114**		**-0.092**
gi|3088341	RS21	ribosomal protein S21	1.481	2					**2.799**
gi|29839750	AT1A3	Sodium/potassium-transporting ATPase alpha-3 chain (Sodium pump 3) (Na+/K+ ATPase 3) (Alpha(III))	1.386	2			**2.114**		**-0.994**
gi|57160805	SH3L1	SH3 domain binding glutamic acid-rich protein like	1.368	2		-0.316			**2.355**
gi|37514845	NUDC1	NudC domain containing 1	1.349	2	**2.130**		-0.422		**0.000**
gi|55661047	RRBP1	ribosome binding protein 1 homolog 180kDa (dog)	1.323	2				-0.240	**2.066**
gi|57162423	5NTD	5'-nucleotidase, ecto (CD73)	1.271	4	**4.652**	**2.585**			**1.392**
gi|984325	6PGD	phosphogluconate dehydrogenase	1.148	3					**2.775**

Proteins measured in 1 biologic replicate only, but in 2 technical replicates

gi|435476	K1C9	cytokeratin 9	33.818		**10.613**	**8.434**			
gi|57864582	HORN	hornerin	17.710		**7.367**	**8.212**			
gi|435675	MT1X	MT-1l protein	4.544		**4.275**	**3.971**			
gi|345829	*[5]	ubiquitin carrier protein E2 - human	3.684		**4.948**	**2.154**			
gi|5902146	UBE2C	ubiquitin-conjugating enzyme E2C isoform 1	3.438		**2.942**	**3.808**			
gi|57208424	CRNL1	Crn, crooked neck-like 1 (Drosophila)	3.131		0.861	**5.404**			
gi|52352803	ZNT1	solute carrier family 30 (zinc transporter), member 1	2.644		**2.504**	**2.827**			
gi|5817162	DREB	hypothetical protein	2.577		1.882	**3.317**			
gi|36327	METK2	S-adenosylmethionine synthetase	2.355		**2.697**	**2.007**			
gi|4507711	TTC1	tetratricopeptide repeat domain 1	2.316		1.692	**2.932**			
gi|4529892	HSP71	HSP70-2	1.949		1.590	**2.101**			
gi|4689140	GBRL2	ganglioside expression factor 2 homolog	1.932		**2.350**	1.285			
gi|56207188	SSU72	novel protein (HSPC182)	1.759		**2.213**	0.915			
gi|20986531	MK01	mitogen-activated protein kinase 1	1.738		1.011	**2.064**			
gi|21619574	OSGEP	O-sialoglycoprotein endopeptidase	1.711		**1.971**	1.011			
gi|54696790	PRAF1	Rab acceptor 1 (prenylated)	1.644		**2.075**	0.688			

Proteins measured only once

gi|13650074	HBA	hemoglobin alpha-1 globin chain	121.222		**13.028**			
gi|18418633	HBB	mutant beta-globin	47.517			**8.781**		
gi|38788274	BPTF	fetal Alzheimer antigen isoform 1	30.503			**7.770**		
gi|4885215	ERBB4	v-erb-a erythroblastic leukemia viral oncogene homolog 4 isoform JM-a/CVT-1 precursor	25.424	**8.724**				
gi|181402	K22E	epidermal cytokeratin 2	18.987	**7.942**				
gi|55958235	MARH5	ring finger protein 153	16.959		**7.702**			
gi|10440389	Q9H7N8	FLJ00030 protein	16.475			**6.366**		
gi|31815	DHE4	glutamate dehydrogenase (NAD(P)+)	15.471		**7.454**			
gi|19923667	RSAD2	radical S-adenosyl methionine domain containing 2	14.315			**6.046**		
gi|34416	TRFL	precursor (AA -19 to 692)	14.032			**6.000**		
gi|13623477	WDR4	WD repeat domain 4	13.968		**7.177**			
gi|2183299	AL1A1	aldehyde dehydrogenase 1	12.845		**6.950**			
gi|4557701	K1C17	keratin 17	12.223					**6.641**
gi|34190642	TRXR3	TXNRD3 protein	12.096		**6.787**			
gi|38541654	Q53YJ2	Dermcidin	9.891		**6.242**			
gi|7688699	Q9P0H9	RER1 protein	9.749	**6.156**				
gi|51470993	*	PREDICTED: similar to sucb isoform 1	9.129	**5.980**				
gi|51467148	*	PREDICTED: similar to tropomyosin 4	9.005		**5.988**			
gi|4557325	APOE	apolipoprotein E precursor	8.927			**4.969**		
gi|9437341	Q9NRV0	x 004 protein	7.502			**4.573**		
gi|1911770	NCOR2	T3 receptor-associating cofactor-1; TRAC-1	7.469	**5.442**				
gi|609308	TCPG	cytoplasmic chaperonin hTRiC5	7.181	**5.337**				
gi|27734452	RAB15	Ras-related protein Rab-15	6.862		**5.252**			
gi|4186185	VIPAR	unknown	6.835			**4.361**		
gi|3075509	PLK2	serum-inducible kinase	6.041			**4.080**		
gi|22671717	HBA	hemoglobin alpha-2	5.865			**4.012**		
gi|541678	D3DTU3	hbZ17	5.798			**3.986**		
gi|57162615	ANK3	ankyrin 3, node of Ranvier (ankyrin G)	5.631			**3.919**		
gi|17390794	TISB	Zinc finger protein 36, C3H type-like 1	5.303			**3.783**		
gi|40788366	TM63A	KIAA0792 protein	4.782				**4.367**	
gi|115143	BTF3	Transcription factor BTF3 (RNA polymerase B transcription factor 3)	4.745		**4.253**			
gi|3763907	RBP56	RBP56/hTAFII68	4.704					**4.006**
gi|49065664	KATNAL2	katanin p60 subunit A-like 2	4.627	**4.160**				

gi|56204086	D3DVZ4	C20orf16	4.450	**4.055**				
gi|28559080	SMOX	polyamine oxidase isoform 4	3.868		**3.700**			
gi|55666285	LCN1L1	lipocalin 1-like 1	3.808					**3.473**
gi|14043853	KITH	Thymidine kinase 1, soluble	3.803			**3.024**		
gi|55664988	KHDR1	KH domain containing, RNA binding, signal transduction associated 1	3.641				**3.591**	
gi|51477696	PARVB	parvin, beta isoform a	3.628	**3.508**				
gi|14602868	GLTP	Glycolipid transfer protein	3.597	**3.485**				
gi|56417844	ARK73	aldo-keto reductase family 7, member A3 (aflatoxin aldehyde reductase)	3.546			**2.865**		
gi|11036646	H2BFS	H2B histone family, member S	3.521				**3.495**	
gi|56404694	RIOK3	Serine/threonine-protein kinase RIO3 (RIO kinase 3) (sudD homolog)	3.133			**2.583**		
gi|40548422	CHM4A	chromatin modifying protein 4A	3.130					**3.516**
gi|386849	K2C6B	keratin type II	3.115		**3.113**			
gi|39843342	A16L1	APG16L beta	3.090			**2.551**		
gi|27657357	Q861B7	MHC class I antigen	2.933	**2.939**				
gi|3559910	CMC1	aralar1	2.916	**2.923**				
gi|37515270	MACD1	LRP16 protein	2.867			**2.381**		
gi|5815178	TX264	unknown	2.855					**3.557**
gi|1143492	GRP78	BiP	2.846	**2.858**				
gi|453155	K1C9	keratin 9	2.792					**3.482**
gi|13937792	Q6FG85	Eukaryotic translation initiation factor 1B	2.778			**2.309**		
gi|1296662	PLEC1	plectin	2.721				**2.761**	
gi|50949925	Q6AI07	hypothetical protein	2.685					**3.348**
gi|9931112	Q9GJF2	human leucocyte antigen Cw	2.659		**2.685**			
gi|55665435	B4DEB1	H3 histone, family 3A	2.659			**2.209**		
gi|47682981	GRPE2	GrpE-like 2, mitochondrial (E. coli)	2.619			**2.175**		
gi|6730096	PAI1	Chain D, Plasminogen Activator Inhibitor-1	2.619	**2.635**				
gi|4758544	HNRNPC	heterogeneous nuclear ribonucleoprotein C isoform b	2.587		**2.610**			
gi|24659879	PRDX2	Peroxiredoxin 2	2.562			**2.124**		
gi|7209305	MRP7	FLJ00002 protein	2.518			**2.085**		
gi|4826774	UCRP	interferon, alpha-inducible protein (clone IFI-15K)	2.504	**2.515**				
gi|7020602	MTMRC	unnamed protein product	2.495			**2.064**		
gi|2143260	P3C2A	phosphoinositide 3-kinase	2.454	**2.461**				
gi|22760981	Q8NC04	unnamed protein product	2.331		**2.329**			
gi|48145713	Q6IBK5	GTF2F1	2.267	**2.249**				
gi|55959755	RPL29	ribosomal protein L29	2.261				**2.233**	

gi|33357878	DCK	Chain B, Structure Of Human Dck Complexed With Gemcitabine And Adp-Mg	2.167	**2.131**			
gi|56205909	RAB4A	RAB4A, member RAS oncogene family	2.166	**2.130**			
gi|4240137	PCF11	KIAA0824 protein	2.136	**2.093**			
gi|38516	CAV1	caveolin	2.091		**2.010**		
gi|2924620	SPIT2	hepatocyte growth factor activator inhibitor type 2	2.044			**2.415**	
gi|642239	1C03	class I histocompatibility antigen HLA-CW3	1.866			**2.104**	
gi|825616	ACTB	unnamed protein product	1.819			**2.017**	

[1] Protein included if at least ½ of biologic z-score values ≥ 1.960σ (indicated by **bold**) and no major disagreements between technical replicates A and B.

[2] 2D-HPLC runs; A and B refer to 2 technical replicates of 3rd biologic sample; 2DLC1 and 2DLC2 refer to 1st and 2nd 2D-HPLC runs.

[3] L:H Ratio refers to geometric mean of all $\log_2$L:H values for each given gi number, expressed as relative protein quantity in infected cultures.

[4] Z-scores from multiple SDS-PAGE fractions collapsed into single most significant value for clarity.

[5] *; Unable to map; record obsolete or removed.

Table 3. A549 proteins decreased > 95% confidence[1]

Accession	HGNC ID	Name	L:H Ratio[3]	Biol. Reps.	Z Score				
					2D-HPLC/MS[2]				SDS-PAGE
					A	B	2DLC1	2DLC2	
Proteins measured in more than 1 biologic replicate									
gi|27597059	DNJC9	DnaJ homolog, subfamily C, member 9	0.009	2	-0.155	-0.554	**-21.013**		
gi|50949588	LS14A	hypothetical protein	0.009	2	-0.279			**-26.334**	
gi|13124770	VKOR1	vitamin K epoxide reductase complex, subunit 1 isoform 1	0.009	2		**-24.902**			**-0.409**
gi|37181648	WDR82	WD40 protein	0.011	2	0.593	0.061	**-21.013**		
gi|5821389	8ODP	MTH1a-Met83 (p26), MTH1b-Met83 (p22), MTH1c-Met83 (p21), MTH1d-Met83 (p18)	0.012	2		**-24.902**			**1.014**
gi|55665273	B9EKV4	aldehyde dehydrogenase 9 family, member A1	0.057	2			-0.371	**-15.994**	
gi|45827757	TACC2	transforming, acidic coiled-coil containing protein 2 isoform a	0.074	2	**-24.615**	-1.545	-0.726		
gi|5726629	SNX12	sorting nexin 12	0.227	2	-0.712	-0.442	**-6.243**		
gi|38511857	GSLG1	Golgi apparatus protein 1	0.342	2	**-3.394**	**-4.634**			**-2.215**
gi|9910266	KIF15	kinesin family member 15	0.344	2	-1.462	**-2.124**	**-3.330**		
gi|33563340	MYH14	myosin, heavy polypeptide 14	0.358	2	**-3.286**		-1.859		
gi|20384898	CTNB1	beta-catenin	0.374	3			**-5.387**	-1.942	**0.164**
gi|5138999	NDUS3	NADH-Ubiquinone reductase	0.416	2	-1.260	**-2.098**	**-2.564**		
gi|47678533	GTPB1	GTPBP1	0.425	2	-1.776		**-2.361**		
gi|55962101	IF4G3	eukaryotic translation initiation factor 4 gamma, 3	0.443	2	**-2.085**	-1.532	**-2.157**		
gi|51479145	BIG1	brefeldin A-inhibited guanine nucleotide-exchange protein 1	0.461	2		**-2.619**	-1.315		
gi|21961441	STRN4	Striatin, calmodulin binding protein 4	0.537	2	**-4.143**		0.721		
gi|763122	RAB35	ray	0.572	2	-1.786	**-2.023**			**-1.110**
gi|7582292	Q9NZE6	BM-010	0.576	2	-0.332	-1.135			**-2.369**
gi|4886522	Q75MJ1	hypothetical protein	0.584	2	**-3.130**		0.236		
gi|32698702	HECTD1	HECT domain containing 1	0.605	2	**-3.042**	-1.500	-0.345		
gi|21752190	Q8N9Z3	unnamed protein product	0.606	2			0.654		**-4.459**
gi|4098297	IF2B3	Koc1	0.610	2	**-1.988**	-1.796			**-0.947**
gi|520587	KPCD	protein kinase C delta-type	0.611	2			**-2.028**	-0.387	

gi|27881820	UN45A	Unc-45 homolog A (C. elegans)	0.638	2		0.073	**-2.099**		
gi|12803105	NUCB1	Nucleobindin 1	0.656	4	**-2.422**	**-2.116**	1.074	**-2.188**	**-1.659**
gi|28422560	NUP53	NUP35 protein	0.700	2	**-2.049**	-1.554			**-0.096**
gi|7022606	PPME1	unnamed protein product	0.716	2			0.043	**-2.070**	
gi|4808278	ERG7	lanosterol synthase	0.721	2	-0.973	**-2.703**	0.081		
gi|6563210	NSF1C	p47 protein	0.722	2					**-2.753**
gi|57014043	Q5I6Y6	lamin A/C transcript variant 1	0.756	3	**-2.320**	**-2.094**			**-0.199**
gi|36155	RIR2	small subunit ribonucleotide reductase	0.759	2	-1.575	**-2.115**	0.322		
gi|5726310	1433G	14-3-3 gamma protein	0.812	2					**-2.185**
gi|913174	LAP2A	TRPP	0.847	3			-0.325		**-2.416**
gi|54648253	FUBP2	KHSRP protein	0.950	6	-0.349	-0.068	0.893	-0.222	**-1.970**

Proteins measured in 1 biologic replicate only, but in 2 technical replicates

gi|5837964	Q564D3	endothelial protein C receptor	0.0001	1	**-24.615**	**-24.902**
gi|18490620	EPCR	Splicing factor, arginine/serine-rich 7, 35kDa	0.0001	1	**-24.615**	**-24.902**
gi|21361822	NDUFA13	NADH dehydrogenase (ubiquinone) 1 alpha subcomplex 13	0.0020	1	**-8.653**	**-24.902**
gi|56550065	CPLX2	complexin 2	0.0055	1	**-24.615**	**-3.229**
gi|30354483	NAA40	N-acetyltransferase 11	0.0063	1	**-2.436**	**-24.902**
gi|34530730	BTBDB	unnamed protein product	0.0064	1	**-2.376**	**-24.902**
gi|55960776	D3DVC8	mitochondrial ribosomal protein L24	0.0065	1	**-2.290**	**-24.902**
gi|4504009	AGAL	galactosidase, alpha	0.0081	1	-1.051	**-24.902**
gi|7657671	UBF1	upstream binding transcription factor, RNA polymerase I	0.209	1	**-3.494**	**-4.840**
gi|29791720	MET10	METT10D protein	0.223	1	**-3.919**	**-4.080**
gi|39645799	Q6P3U7	RXRA protein	0.278	1	**-3.678**	**-3.131**
gi|6730223	PROF2	Chain D, Crystal Structure Of Human Profilin Ii	0.284	1	-0.987	**-5.718**
gi|4503453	EDF1	endothelial differentiation-related factor 1 isoform alpha	0.297	1	**-4.678**	-1.759
gi|55960673	D3DPX7	protein tyrosine phosphatase, receptor type, F	0.313	1	**-3.252**	**-2.916**
gi|25987321	Q54A15	URP1	0.324	1	**-2.317**	**-3.669**

gi|55770850	CP24A	cytochrome P450, family 24 precursor	0.364	1	**-2.915**	**-2.427**
gi|23512254	SF01	SF1 protein	0.379	1	**-2.849**	**-2.284**
gi|27769298	TRI25	Tripartite motif-containing 25	0.439	1	-1.915	**-2.425**
gi|457262	Q7KZ24	nuclease sensitive element binding protein-1	0.449	1	**-2.011**	**-2.209**
gi|10798851	FADS2	fatty acid desaturase 2	0.472	1	**-2.412**	-1.539
gi|10436660	Q9H7U7	unnamed protein product	0.487	1	**-2.703**	-1.074
gi|34999	CADH2	unnamed protein product	0.487	1	**-2.253**	-1.522
gi|4589628	PALLD	KIAA0992 protein	0.487	1	**-2.653**	-1.117
gi|4503131	CTNNB1	catenin (cadherin-associated protein), beta 1, 88kDa	0.487	1	**-2.154**	-1.621
gi|14124936	CO044	Chromosome 15 open reading frame 44	0.491	1	-1.782	**-1.960**
gi|6492130	D3DU08	urokinase receptor-associated protein uPARAP	0.491	1	-1.359	**-2.386**
gi|2865163	TGFI1	Hic-5	0.499	1	**-2.376**	-1.271
gi|4506409	RANBP3	RAN binding protein 3 isoform RANBP3-a	0.505	1	**-2.390**	-1.189
gi|4759068	SCO1	cytochrome oxidase deficient homolog 1	0.507	1	-1.395	**-2.177**
gi|27477134	PO210	nucleoporin 210	0.509	1	**-2.405**	-1.135
gi|7657683	XCT	solute carrier family 7, (cationic amino acid transporter, y+ system) member 11	0.542	1	**-2.229**	-0.972

Proteins measured only once

gi|49899808	RHG05	ARHGAP5 protein	0.0001	1		**-21.013**
gi|47115211	ARL3	ARL3	0.0001	1		**-26.334**
gi|5326759	KCC2B	calcium/calmodulin-dependent protein kinase II beta e' subunit	0.0001	1		**-21.013**
gi|8571386	ICLN	chloride ion current inducer protein I(Cln)	0.0001	1		**-26.334**
gi|51594277	Q670S4	hemoglobin Lepore-Baltimore	0.0001	1		**-21.013**
gi|21739669	IWS1	hypothetical protein	0.0001	1		**-21.013**
gi|21739912	HTR7A	hypothetical protein	0.0001	1		**-21.013**
gi|34365494	CE044	hypothetical protein	0.0001	1		**-21.013**
gi|57997169	Q5JPD9	hypothetical protein	0.0001	1		**-21.013**

gi|57471655	KDM5C	Jumonji, AT rich interactive domain 1C (RBP2-like)	0.0001	1			**-21.013**
gi|6382020	RHG31	KIAA1204 protein	0.0001	1			**-21.013**
gi|56081771	DUSTY	Receptor interacting protein kinase 5	0.0001	1			**-21.013**
gi|55960721	VAV3	vav 3 oncogene	0.0001	1			**-21.013**
gi|23903	MK04	63kDa protein kinase	0.0001	1		**-24.902**	
gi|29727	MYH7	cardiac beta myosin heavy chain	0.0001	1		**-24.902**	
gi|25990944	CLIC6	chloride channel form B	0.0001	1	**-24.615**		
gi|2828149	PPIE	cyclophilin-33A	0.0001	1		**-24.902**	
gi|115855	CBL	E3 ubiquitin-protein ligase CBL (Signal transduction protein CBL) (Proto-oncogene c-CBL) (Casitas B-lineage lymphoma proto-oncogene) (RING finger protein 55)	0.0001	1		**-24.902**	
gi|6942004	EHD3	EH domain containing protein 2	0.0001	1	**-24.615**		
gi|18676696	MOV10	FLJ00247 protein	0.0001	1	**-24.615**		
gi|42407269	HELLS	lymphoid specific helicase variant8	0.0001	1		**-24.902**	
gi|20986521	MK08	mitogen-activated protein kinase 8 isoform 4	0.0001	1		**-24.902**	
gi|3041706	MYH6	Myosin heavy chain, cardiac muscle alpha isoform (MyHC-alpha)	0.0001	1		**-24.902**	
gi|55664366	STRBP	spermatid perinuclear RNA binding protein	0.0001	1	**-24.615**		
gi|5454100	TACC1	transforming, acidic coiled-coil containing protein 1	0.0001	1		**-24.902**	
gi|35438	PGK2	unnamed protein product	0.0001	1	**-24.615**		
gi|13124617	VTI1B	Vesicle transport through interaction with t-SNAREs homolog 1B (Vesicle transport v-SNARE protein Vti1-like 1) (Vti1-rp1)	0.0001	1		**-24.902**	
gi|7020344	MIO	unnamed protein product	0.022	1			**-8.672**

gi|46250008	PP4R4	KIAA1622	0.108	1			**-5.090**		
gi|51859376	H33	H3 histone, family 3A	0.131	1					**-5.138**
gi|46249414	LTBP1	latent transforming growth factor beta binding protein 1 isoform LTBP-1L	0.148	1			**-4.380**		
gi|576554	ANT3	antithrombin III variant	0.187	1			**-3.841**		
gi|21264337	ARAP3	centaurin, delta 3	0.228	1			**-3.391**		
gi|4557707	L1CAM	L1 cell adhesion molecule isoform 1 precursor	0.243	1			**-3.244**		
gi|55664563	KI67	antigen identified by monoclonal antibody Ki-67	0.253	1	**-3.626**				
gi|39932736	MYO5B	Myosin-5B (Myosin Vb)	0.265	1			**-3.046**		
gi|31127073	RANB9	RANBP9 protein	0.266	1			**-3.038**		
gi|7023521	FBX3	unnamed protein product	0.275	1			**-2.964**		
gi|40788219	NRCAM	KIAA0343	0.277	1		**-3.443**			
gi|190133	AT2B1	plasma membrane Ca2+ pumping ATPase	0.279	1		**-3.420**			
gi|16741274	Q53SZ8	Prolactin regulatory element binding	0.279	1			**-2.929**		
gi|3413793	NB5R3	NADH-cytochrome b5 reductase	0.281	1					**-3.759**
gi|51467774	RPS3AP5	PREDICTED: similar to ribosomal protein S3a isoform 1	0.289	1					**-3.121**
gi|6468766	LCAP	oxytocinase/insulin-responsive aminopeptidase, variant 1	0.292	1			**-2.827**		
gi|22761383	CAB45	unnamed protein product	0.304	1	**-3.132**				
gi|55859586	NU188	nucleoporin 188kDa	0.304	1			**-2.732**		
gi|55664592	ARGAL	novel protein	0.319	1			**-2.625**		
gi|10799803	RBSK	ribokinase	0.321	1			**-2.608**		
gi|6983729	MYL9	MYL9	0.325	1		**-3.007**			
gi|21311254	STXB6	amisyn	0.330	1			**-2.546**		
gi|5689473	NUDC3	KIAA1068 protein	0.337	1			**-2.497**		
gi|45501300	Q6NXG4	WDR13 protein	0.338	1			**-2.491**		
gi|23273305	D3DS37	Jub, ajuba homolog (Xenopus laevis)	0.338	1			**-2.490**		
gi|1685075	PTPRJ	density enhanced phosphatase-1	0.342	1	**-2.817**				
gi|22902182	RAVR1	RAVER1 protein	0.348	1			**-2.425**		
gi|57160661	MIPEP	mitochondrial intermediate peptidase	0.355	1			**-2.380**		
gi|27764863	SLC25A6	solute carrier family 25, member A6	0.355	1	**-2.716**				
gi|50949497	ALO17	hypothetical protein	0.364	1		**-2.700**			
gi|15559717	AP2A1	AP2A1 protein	0.368	1				**-2.941**	
gi|115351	CO5A2	Collagen alpha-2(V) chain precursor	0.381	1			**-2.222**		
gi|55960069	CJ076	novel protein	0.387	1			**-2.185**		
gi|21706672	CRIP2	Cysteine-rich protein 2	0.387	1		**-2.531**			
gi|31874098	NRCAM	hypothetical protein	0.388	1	**-2.477**				

gi|45501252	PRAX	Periaxin	0.389	1				**-2.780**	
gi|20306890	PSA7L	Proteasome (prosome, macropain) subunit, alpha type, 8	0.392	1		**-2.500**			
gi|57162346	DIAPH3	diaphanous homolog 3 (Drosophila)	0.392	1			**-2.154**		
gi|292870	UFO	tyrosine kinase receptor	0.392	1		**-2.497**			
gi|53791223	FINC	fibronectin 1	0.403	1			**-2.094**		
gi|55957730	D3DVE6	WD repeat domain 42A	0.404	1			**-2.084**		
gi|48429194	UFO	Tyrosine-protein kinase receptor UFO precursor (AXL oncogene)	0.407	1	**-2.351**				
gi|12804489	MELPH	Melanophilin	0.412	1	**-2.318**				
gi|178743	APEX1	apurinic endonuclease	0.415	1		**-2.347**			
gi|56204680	Q5T8R3	solute carrier family 16 (monocarboxylic acid transporters), member 1	0.418	1					**-3.006**
gi|15488917	PRKCSH	protein kinase C substrate 80K-H	0.420	1		**-2.311**			
gi|57209070	Q5JTE2	RP3-337H4.4	0.421	1			**-1.994**		
gi|34531906		unnamed protein product	0.425	1		**-2.280**			
gi|48255937	CD44	CD44 antigen isoform 2 precursor	0.425	1					**-2.946**
gi|1575607	FUBP2	FUSE binding protein 2	0.431	1					**-2.901**
gi|6969149	MCM3	MCM3 minichromosome maintenance deficient 3 (S. cerevisiae)	0.436	1					**-2.069**
gi|39753961	IQGA3	IQ motif containing GTPase activating protein 3	0.444	1		**-2.160**			
gi|18860900	PTPRJ	protein tyrosine phosphatase, receptor type, J precursor	0.448	1		**-2.136**			
gi|56204524	ARPC5	actin related protein 2/3 complex, subunit 5, 16kDa	0.449	1					**-2.764**
gi|55665466	D3DV57	novel protein (FLJ21919)	0.451	1					**-1.985**
gi|55665798	UBP2L	ubiquitin associated protein 2-like	0.471	1		**-2.000**			
gi|50949942	S4A7	hypothetical protein	0.477	1		**-1.966**			
gi|1184699	SYYC	tyrosyl-tRNA synthetase	0.479	1					**-2.149**
gi|30268334	CD44	hypothetical protein	0.479	1					**-2.148**

[1] Protein included if at least ½ of biologic z-score values ≤ -1.960σ (indicated by **bold**) and no major disagreements between technical replicates A and B.

[2] 2D-HPLC runs; A and B refer to 2 technical replicates of 3rd biologic sample; 2DLC1 and 2DLC2 refer to 1st and 2nd 2D-HPLC runs.

[3] L:H Ratio refers to geometric mean of all $\log_2$L:H values for each given gi number, expressed as relative protein quantity in infected cultures.

[4] Z-scores from multiple SDS-PAGE fractions collapsed into single most significant value for clarity.

[5] *; Unable to map; record obsolete or removed.

Figure 1

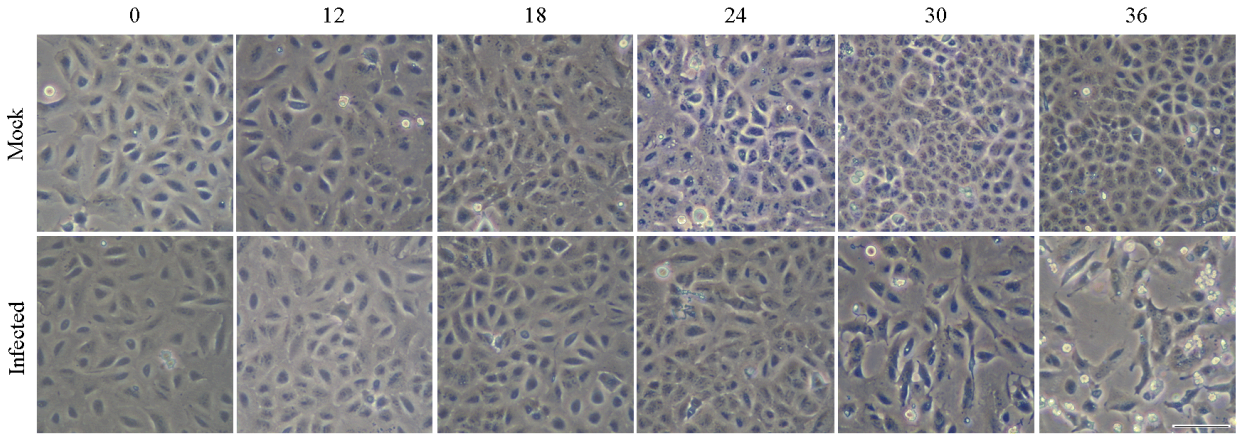

Figure 2

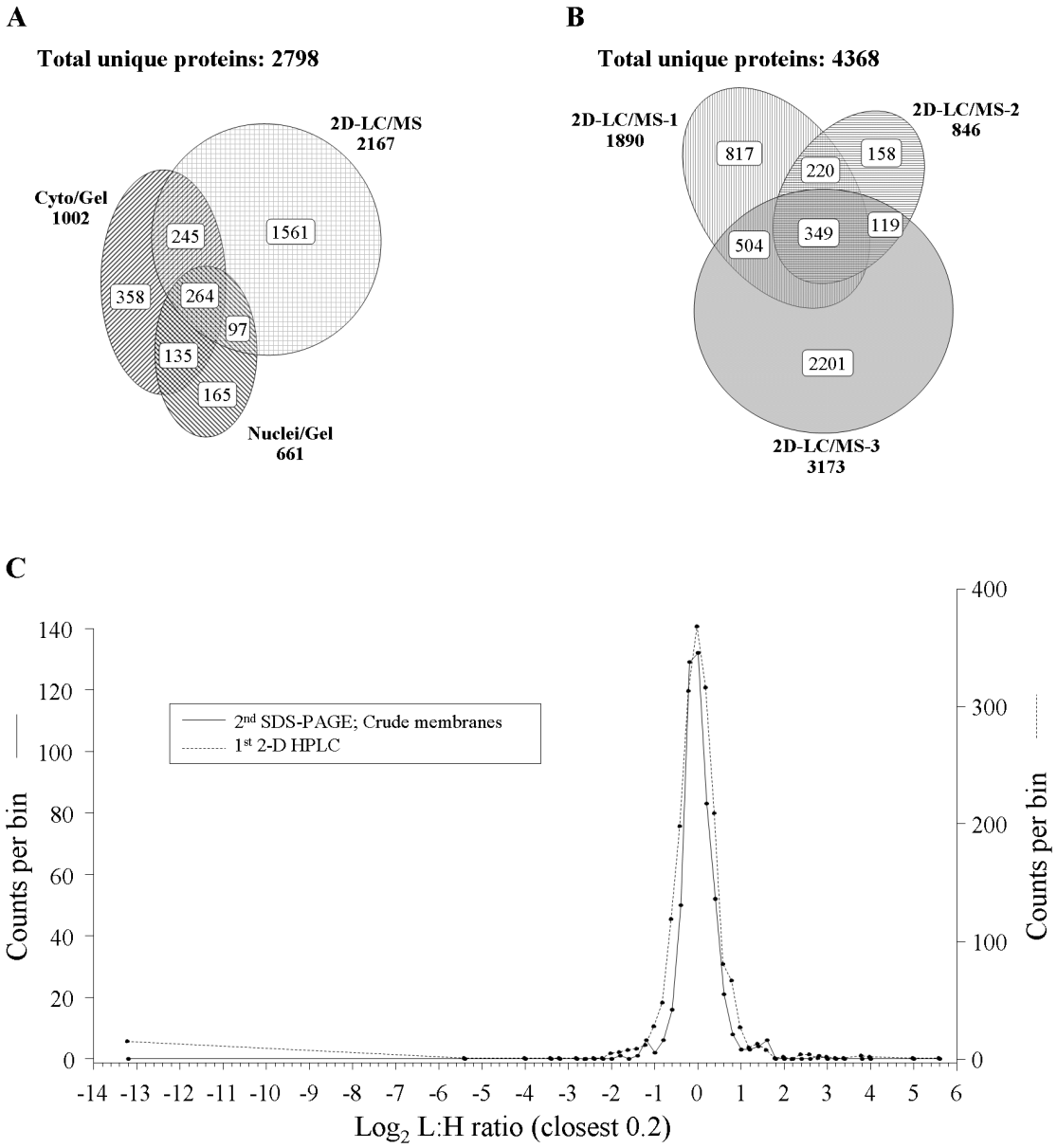

Figure 3

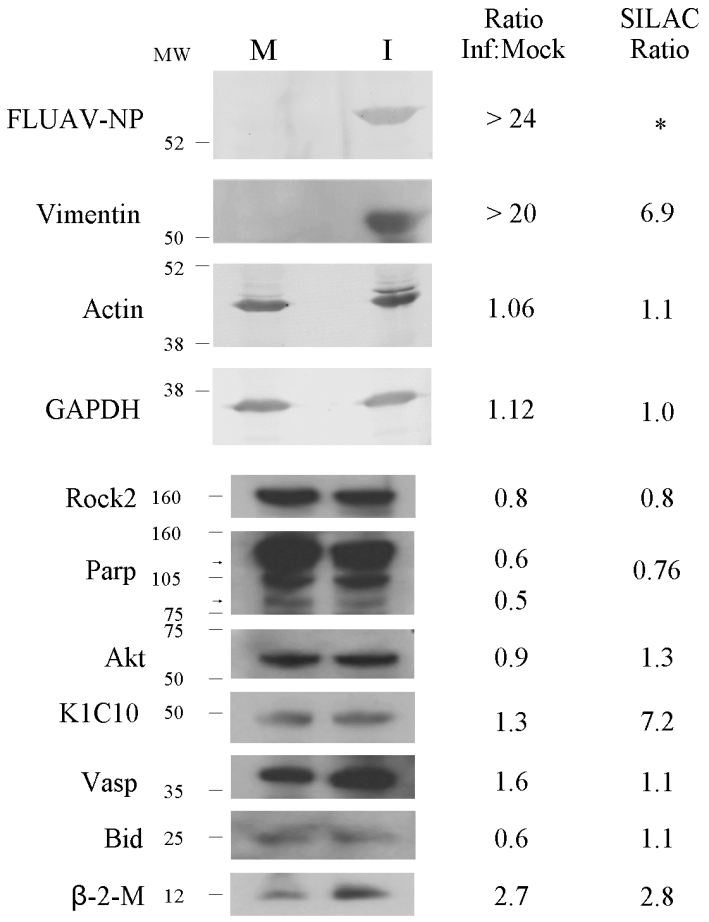

Figure 4

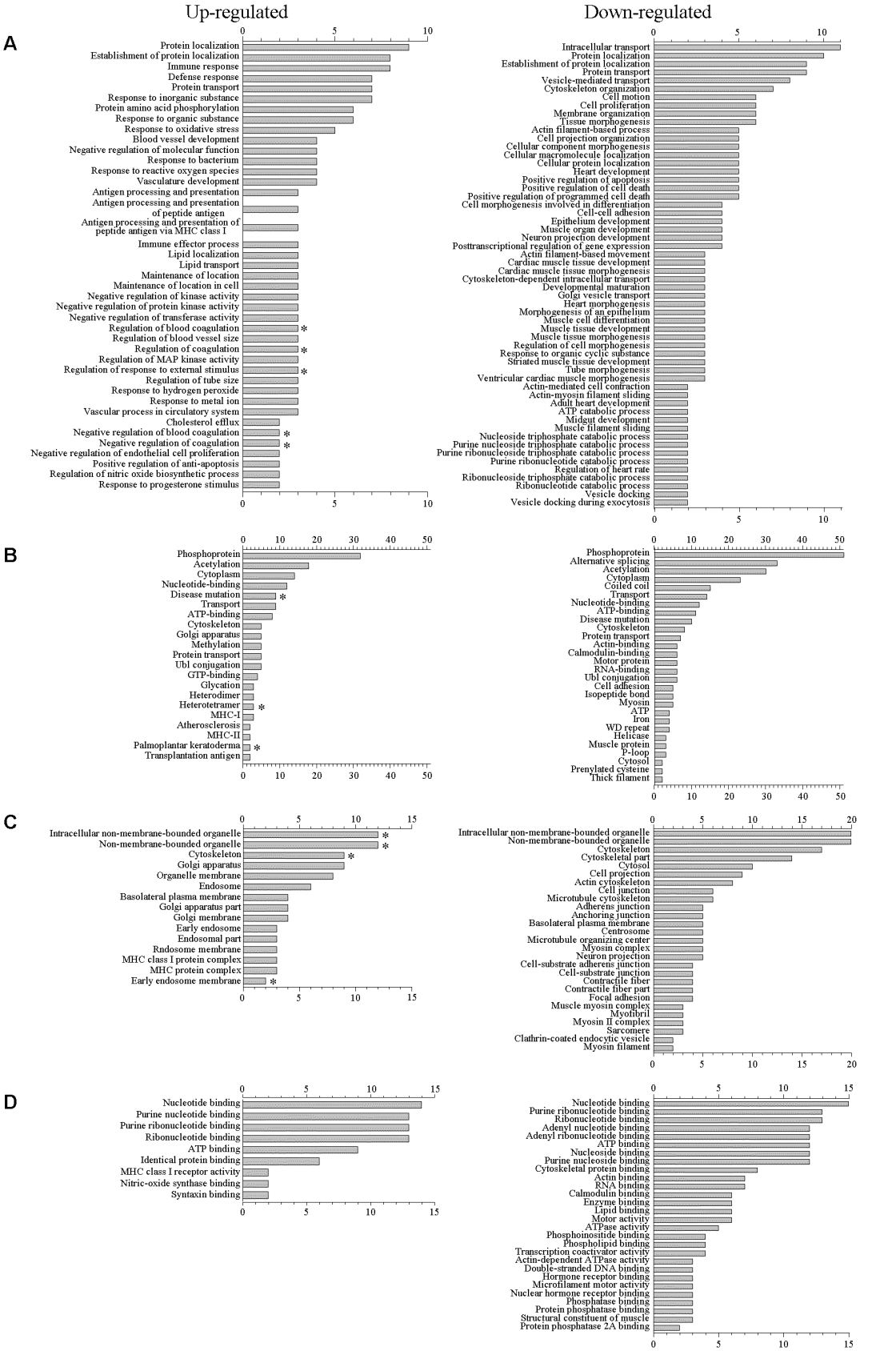

Figure 5